

Scattering of Glue by Glue on the Light-cone Worldsheet I: Helicity Non-conserving Amplitudes ¹

D. Chakrabarti², J. Qiu³, and C. B. Thorn⁴

*Institute for Fundamental Theory
Department of Physics, University of Florida, Gainesville FL 32611*

Abstract

We give the light-cone gauge calculation of the one-loop on-shell scattering amplitudes for gluon-gluon scattering which violate helicity conservation. We regulate infrared divergences by discretizing the p^+ integrations, omitting the terms with $p^+ = 0$. Collinear divergences are absent diagram by diagram for the helicity non-conserving amplitudes. We also employ a novel ultraviolet regulator that is natural for the light-cone worldsheet description of planar Feynman diagrams. We show that these regulators give the known answers for the helicity non-conserving one-loop amplitudes, which don't suffer from the usual infrared vagaries of massless particle scattering. For the maximal helicity violating process we elucidate the physics of the remarkable fact that the loop momentum integrand for the on-shell Green function associated with this process, with a suitable momentum routing of the different contributing topologies, is identically zero. We enumerate the counterterms that must be included to give Lorentz covariant results to this order, and we show that they can be described locally in the light-cone worldsheet formulation of the sum of planar diagrams.

¹Supported in part by the Department of Energy under Grant No. DE-FG02-97ER-41029.

²E-mail address: dipankar@phys.ufl.edu

³E-mail address: jqiu@phys.ufl.edu

⁴E-mail address: thorn@phys.ufl.edu

1 Introduction and Conclusion

The lightcone worldsheet representation of the sum of the planar diagrams of quantum field theory [1, 2] shows a sense in which the string/field duality proposed by Maldacena [3] for the case of certain supersymmetric gauge theories can be universally valid for almost any field theory. However, unlike the $\mathcal{N} = 4$ supersymmetric gauge theory initially studied by Maldacena, a general quantum field theory has ultraviolet divergences that can complicate (or possibly ruin) the string description. Indeed the generic worldsheet representation proposed in [2] applies directly only to the bare diagrams of the quantum field theory, and one must apply an explicit *UV* cutoff to give it concrete meaning. Since any physical cutoff will break Lorentz invariance, there is the danger that the counterterms required to restore it may not be compatible with a *local* worldsheet description.

For the case of cubic scalar field theory in six space-time dimensions (the marginally renormalizable situation), a study of the divergence structure has confirmed that every counterterm required for the restoration of Lorentz invariance has a viable local worldsheet interpretation [4]. In that work, it was shown that two counterterms beyond the ones associated with mass, wave-function, and coupling renormalization were required. But it turned out that they only contributed to the self-energy diagrams: one could be interpreted as a simple rescaling of the worldsheet action (or alternatively as a renormalization of the speed of light), while the other new counterterm represented a modification of the boundary conditions enjoyed by the worldsheet fields. Both of these new counterterms are compatible with a local worldsheet dynamics.

It would be highly desirable to extend this all orders conclusion to the worldsheet description of gauge theories, such as the gauge sector of QCD [5]. Unfortunately, because we work in light-cone gauge, the corresponding analysis is considerably more complex, and we are still short of a complete all orders result. However, we have completed the one loop analysis and describe it in a series of two articles. In this one we calculate the helicity amplitudes with helicity nonconservation. Since the tree amplitudes for such processes vanish, the one-loop amplitudes are finite in both the ultraviolet and infrared. In the sequel we shall deal with the helicity conserving amplitudes which suffer from infrared divergences.

While the literature has dealt with one-loop coupling renormalization in light-cone gauge including confirmation of asymptotic freedom [6, 7], a check of Lorentz invariance at one loop requires the complete evaluation, including all finite contributions, of the amplitudes for a manifestly physical scattering process. The simplest such process is the on-shell scattering of glue by glue, and a complete light-cone gauge calculation of this process is, to our knowledge, unavailable. We offer such a calculation in this work, using the worldsheet friendly ultraviolet cutoff employed in [4].

For the reader unfamiliar with [4] we briefly describe here how this cutoff is implemented. The worldsheet formalism maps the sum of planar diagrams (singled out in $SU(N_c)$ gauge theory, for example, by 't Hooft's large N_c limit [1]) to a rectangular worldsheet whose length and width are light-cone time and longitudinal momentum respectively. To study this mapping in perturbation theory, it suffices to use a regulator that exploits the planarity of the diagrams. A general planar diagram can be drawn on a plane with external lines extending to infinity (see Fig. 1). The internal and external lines divide the plane into regions. Loops bound finite regions in the plane and external lines bound regions extending to infinity. The worldsheet description of planar diagrams [1, 2] employs "dual momentum" variables, q_i for finite regions and k_j for external regions, one for each region as shown in Fig. 1. The actual momentum carried by any line, which separates two regions of the plane, is the difference of the dual momentum variables of those regions⁵. The Feynman diagram is given by an integral over all the q_i . In these variables, the worldsheet friendly ultraviolet cutoff $\delta > 0$ described in [4] is implemented by simply inserting a factor $e^{-\delta \sum_i q_i^2}$ in the loop integrand, where q_i is the transverse dual momentum of the region bounded by loop i . Note that it only cuts off transverse momentum. This is because the worldsheet formalism promotes the transverse dual momenta to worldsheet fields whereas the \pm coordinates merely parametrize the worldsheet.

As already mentioned the physical quantities we calculate in this article are on shell scattering amplitudes.

⁵Since $SU(N_c)$ planar diagrams are orientable, we can establish a unique convention that the momentum carried by the line in a given direction is the dual momentum of the region to the right minus that of the region to the left with respect to someone facing in the direction of momentum flow.

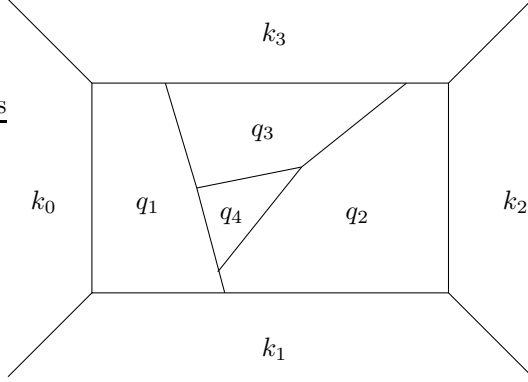


Figure 1: Assignment of dual momentum variables to a planar diagram.

In quantum field theories with massless fields (in particular gauge theories), these quantities have infrared as well as ultraviolet divergences, and we must also regulate these. It is quite natural to define the worldsheet path integral on a lattice [2, 8], and in the lightcone worldsheet description of field theories such a lattice corresponds to discretizing the $+$ component of momenta $p^+ = lm$, $l = 1, 2, \dots$, where $p^\pm \equiv (p^0 \pm p^z)/\sqrt{2}$ [8–10]. We choose to do this, and thereby we regulate all infrared divergences that come from integration regions where all components of a loop momentum are small. But scattering amplitudes also typically have collinear divergences from the regions where an internal momentum is parallel to (collinear with) an on-shell external momentum. These divergences are not regulated by discretization of p^+ . This would be problematic for scalar couplings but for gauge theories, in light-cone gauge, the cubic vertex provides an extra zero that renders the problem manageable. Actually the easiest way to see this uses the light-cone description itself. Consider an on-shell external line with momentum k hooked to two internal lines with momenta $p, p - k$. In a frame where the transverse components $\mathbf{k} = 0$, the propagators of the internal lines supply factors

$$\frac{1}{p^2(p - k)^2} = \frac{1}{(p^2 - 2p^+p^-)(p^2 - 2(p^+ - k^+)p^-)}$$

Integrating this expression near $p, p^- = 0$ shows a logarithmic divergence even if $p^+ \neq 0, k^+$. Happily, the cubic gauge coupling in lightcone gauge supplies a further factor

$$\mathbf{K} = k^+ \mathbf{p} - p^+ \mathbf{k} \rightarrow k^+ \mathbf{p}$$

which gives an additional zero that removes the divergence. As a result the only impact that the collinear divergences have is in the on-shell limit of self-energy corrections. The off-shell ($k^2 \neq 0$) self-energy correction has the small momentum behavior $O(k^2 \ln k^2)$, where the logarithmic cut is associated with threshold for massless gluon production, which occurs in the collinear limit. Since we divide by k^2 to get the wave function renormalization, we see that the latter will have a logarithmic collinear divergence in the on-shell limit $k^2 \rightarrow 0$. Thus, in lightcone gauge, the collinear divergence problem is limited to self-energy bubbles on external lines. But, for the helicity nonconserving amplitudes calculated in this article, such diagrams don't contribute and the problem disappears. In the second article of this series these contributions will be present and will be tied up with the resolution of the physics of soft gluon emission.

Before summarizing the content of this article, there is a final general point about lightcone gauge we wish to mention here. With this gauge choice, only the transverse components of the gauge field \mathbf{A} remain as propagating degrees of freedom. In 4 space-time dimensions, it is convenient to assemble the two transverse components into a complex field $A^\wedge \equiv (A^1 + iA^2)/\sqrt{2}$, with complex conjugate $A^\vee \equiv (A^1 - iA^2)/\sqrt{2}$ represented in Feynman diagrams by attaching an arrow, representing a “charge flow” to each line of the diagram. But what is the physical interpretation of this “charge”? At first glance it seems to be just the

“spin” projected on the z -axis. But this interpretation makes it seem highly frame dependent. A not widely recognized fact is that for an on-shell gluon the “charge” is actually the frame independent helicity of the gluon. The helicity $h = \vec{p} \cdot \vec{J}/|\vec{p}|$ of a massless particle is well-known to be a Lorentz invariant. (Here \vec{p} is the three momentum of the gluon and \vec{J} is the total angular momentum.). It is straightforward to express \vec{p} and \vec{J} in terms of the light-cone components of the Poincaré generators and apply h to a single gluon state and find

$$h[a_1^\dagger(\mathbf{p}, p^+) \pm ia_2^\dagger(\mathbf{p}, p^+)]|0\rangle = \pm[a_1^\dagger(\mathbf{p}, p^+) \pm ia_2^\dagger(\mathbf{p}, p^+)]|0\rangle$$

It follows that the globally defined combinations $(a_1^\dagger(p) \pm ia_2^\dagger(p))/\sqrt{2}$ create one gluon states of helicity ± 1 no matter which direction the gluon is moving! Thus the light-cone Feynman rules in this complex field basis directly give the helicity scattering amplitudes in the on-shell limit. This probably indicates a close connection of the light-cone worldsheet [2] description of gauge theory [5] to the twistor string representation [11, 12] of gauge theory. In the latter work the helicity amplitudes also play a central role. We think it likely that the lightcone worldsheet formalism provides a concrete all orders lightcone gauge fixed realization of the twistor string idea.

We now turn to a synopsis of the rest of the article. In Section 2 we quote the Feynman rules in lightcone gauge. This gauge completely removes the redundant gauge fields A_\pm from the formalism, so the lines of every diagram represent only the transverse components of the gluons. Central to the Feynman rules are the quantities $K_{ij}^\mu = p_i^+ p_j^\mu - p_j^+ p_i^\mu$. In Section 3, we obtain a number of identities enjoyed by the K_{ij} that enable dramatic simplification of the final results for each helicity amplitude. The quantities K_{ij} play the role of the bispinor matrix elements that occur in the famous Parke-Taylor formulas [13] for gluon tree amplitudes.

Section 4 is devoted to the calculation of four gluon tree amplitudes. Tree diagrams with four like helicities cannot even be drawn in light-cone gauge, so their vanishing is guaranteed from the start. The diagrams for tree amplitudes with three like-helicities *can* be drawn and are non-zero off-shell. However the K identities can be used to show that they vanish on-shell. We also obtain the Parke-Taylor forms for the helicity conserving tree amplitudes, though their one-loop corrections are reserved for the second paper in this series.

Section 5 discusses the gluon self energy diagrams. These have been calculated previously in various treatments of lightcone gauge but not with the worldsheet friendly regulator we are employing here. Thus we give the calculation in complete detail. In particular we determine the counterterms required to maintain Lorentz invariance and show that they have a local worldsheet description. In Section 6 we quote the results for the one-loop cubic vertex function with calculational details to be found in [14]. Again we note the counterterms required by Lorentz invariance and give their representation in the worldsheet formalism.

We discuss box diagrams in Section 7. For the helicity nonconserving amplitudes discussed in this paper it turns out that the boxes can all be reduced to a sum of triangle-like diagrams. We show how this reduction takes place and quote the set of triangle-like diagrams descended from the boxes in each case.

Finally in Sections 8 and 9 we put everything together and calculate the on-shell amplitudes for the scattering of glue by glue in the case of four like helicities and three like helicities respectively. The final answer for each of these cases is finite in both the ultraviolet and infrared and agrees with the known answer. In the four like helicity case, every one-loop diagram is finite. However the individual light-cone gauge diagrams combine in a very interesting way. Bern [15] has observed that, if one takes all contributing diagrams to the on-shell one-loop four point Green function, and routes momenta appropriately, the integrands for all these diagrams sum to zero *before* integration. The appropriate momentum routing turns out to be precisely that dictated by the worldsheet description of planar diagrams [2]. In spite of this vanishing integrand, the physical scattering is non-zero, because the helicity flipping self-energy insertions essential for this cancellation to occur are non-zero, and must be removed by counterterms. Thus the physical scattering amplitude is given by the negative of the sum of helicity flipping self energy insertions—a relatively simple calculation! This case serves as a nontrivial test of the validity of one of the counterterms, namely the one that cancels the helicity flipping component of the gluon self-energy diagram. In contrast, the three like helicity case tests much more. The individual diagrams contributing to this process are divergent in both

the ultraviolet and infrared. These divergences cancel in the sum of all contributing diagrams, but all of the counterterms we have determined *must be included to get the long known correct answer* [16, 17]. We mention that our methods for obtaining one-loop scattering amplitudes have some similarity and overlap with those of [18].

It is an important constraint on the all orders validity of the worldsheet description of gauge theories [2, 5] that *all* of the counterterms required to achieve Lorentz invariance can be interpreted as new terms in a *local* worldsheet action. Confirmation of this requirement to one-loop order is the main achievement of the work described here. The second article in this series will extend the one-loop analysis to the IR divergent helicity conserving case. But a complete all orders demonstration that all counterterms have a local lightcone worldsheet interpretation remains a distant goal.

2 Feynman Rules for Light-cone gauge Yang-Mills

We use the notation and conventions in Ref. [19], according to which the values of the non-vanishing three transverse gluon vertices are:

$$\begin{array}{c} \text{Diagram: } \begin{array}{c} \text{up} \\ \diagup \quad \diagdown \\ \text{1} \quad \text{2} \end{array} \end{array} = \frac{2gp_3^+}{p_1^+ p_2^+} (p_1^+ p_2^\wedge - p_2^+ p_1^\wedge) = \frac{2gp_3^+}{p_1^+ p_2^+} K_{12}^\wedge \quad (1)$$

$$\begin{array}{c} \text{Diagram: } \begin{array}{c} \text{up} \\ \diagup \quad \diagdown \\ \text{1} \quad \text{2} \end{array} \end{array} = \frac{2gp_3^+}{p_1^+ p_2^+} (p_1^+ p_2^\vee - p_2^+ p_1^\vee) = \frac{2gp_3^+}{p_1^+ p_2^+} K_{12}^\vee \quad (2)$$

Here, $p_j^\wedge = (p_j^x + ip_j^y)/\sqrt{2}$, $p_j^\vee = (p_j^x - ip_j^y)/\sqrt{2}$, and p_j^+ are the components of the momentum *entering* the diagram on leg j . This coupling constant g differs by a factor of $\sqrt{2}$ from the conventional one $g = g_s/\sqrt{2}$. We remind the reader that these are light-cone gauge ($A_- = 0$) expressions and include the contributions that arise when the longitudinal field A_+ is eliminated from the formalism.

The quartic vertices in this helicity basis are given by

$$\begin{array}{c} \text{Diagram: } \begin{array}{c} \text{up} \\ \diagup \quad \diagdown \\ \diagup \quad \diagdown \\ \text{1} \quad \text{2} \quad \text{3} \quad \text{4} \end{array} \end{array} = -2g^2 \frac{p_1^+ p_3^+ + p_2^+ p_4^+}{(p_1^+ + p_4^+)^2} \quad (3)$$

$$\begin{array}{c} \text{Diagram: } \begin{array}{c} \text{up} \\ \diagup \quad \diagdown \\ \diagup \quad \diagdown \\ \text{1} \quad \text{2} \quad \text{3} \quad \text{4} \end{array} \end{array} = +2g^2 \left(\frac{p_1^+ p_2^+ + p_3^+ p_4^+}{(p_1^+ + p_4^+)^2} + \frac{p_1^+ p_4^+ + p_2^+ p_3^+}{(p_1^+ + p_2^+)^2} \right) \quad (4)$$

where we again stress that these expressions include contributions from the elimination of A_+ . We also should point out that we are giving these rules in the context of the $1/N_c$ expansion, so the planar diagrams of the $SU(N_c)$ theory are correctly given with the simple substitution $g \rightarrow g\sqrt{N_c}$. Non-planar diagrams after this substitution must be accompanied by appropriate powers of $1/N_c^2$, depending on the number of “handles” in the diagram. We have not spelled that out here, because our focus will be on the planar diagrams in this article. The results we obtain should therefore be compared to the ’t Hooft limit $N_c \rightarrow \infty$, fixed $g^2 N_c$ of those in the literature. In making such comparisons, note that the substitution rule $g \rightarrow g\sqrt{N_c}$ multiplies conventionally defined n -gluon tree amplitudes by a factor $N_c^{n/2-1} \rightarrow N_c$ for $n = 4$, so for each gluon scattering process we remove this factor before comparing to the literature.

3 K Identities

As we have seen the quantities

$$K_{ij}^\mu \equiv p_i^+ p_j^\mu - p_j^+ p_i^\mu \quad (5)$$

play a central role in the cubic Yang-Mills vertex. In fact, we shall find that the simplest forms of the various helicity amplitudes are achieved by expressing them as functions of the K 's. These simple forms are in fact identical to those discovered by Parke and Taylor using a bispinor representation of polarization vectors [13]. For us the role of the spinor matrix elements in those formulas will be played exclusively by K_{ij}^\wedge and K_{ij}^\vee .

In order to reduce the expressions for the helicity amplitudes to the Parke-Taylor form, we will need a number of identities enjoyed by the K 's. For a general n -gluon amplitude we can form K_{ij} for each pair of gluons (ij) , where $i, j = 1, \dots, n$ distinguish the different gluons. By momentum conservation, it is immediate that

$$\sum_j K_{ij}^\mu = 0. \quad (6)$$

From the fact that K is an anti-symmetric product we have Bianchi-like identities

$$p_i^+ K_{jk}^\mu + p_k^+ K_{ij}^\mu + p_j^+ K_{ki}^\mu = 0 \quad (7)$$

$$K_{li}^\wedge K_{jk}^\wedge + K_{lk}^\wedge K_{ij}^\wedge + K_{lj}^\wedge K_{ki}^\wedge = 0 \quad (8)$$

Finally, the most powerful type of identity follows from a very simple calculation

$$\sum_j \frac{K_{ij}^\wedge K_{jk}^\vee}{p_j^+} = -p_i^+ p_k^+ \sum_j \frac{p_j^2}{2p_j^+} \quad (9)$$

which seems like a complicated non-linear relation. However when we are considering scattering amplitudes, the momenta all satisfy $p_i^2 = 0$ so the right side is zero! This identity plays a central role in showing that trees with all but one like helicities vanish. The K identities are also crucial for reducing the complexity of the helicity amplitudes that don't vanish.

4 Tree Amplitudes

As a preliminary, we evaluate the $\wedge\wedge\wedge\vee$ four-point tree with one leg off-shell, which will aid the construction of the loop integrand. For definiteness, let the \vee helicity be on leg 4 where legs 1234 are labeled counter-clockwise around the diagram, as shown in Fig. 2. Also we omit the coupling factor $2g$ for each vertex.

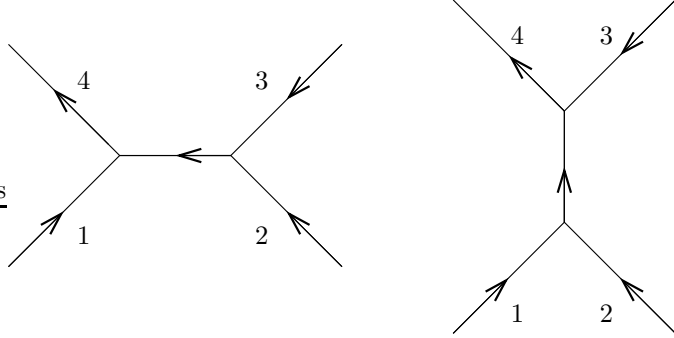


Figure 2: Tree diagrams for the gluon scattering with polarizations $\wedge\wedge\wedge\vee$.

Then

$$A_{tree}^{\wedge\wedge\wedge\vee} = -\frac{p_4^+}{p_1^+ p_2^+ p_3^+} \left[\frac{K_{32}^\wedge K_{44}^\wedge}{(p_2 + p_3)^2} + \frac{K_{43}^\wedge K_{21}^\wedge}{(p_1 + p_2)^2} \right] \quad (10)$$

$$(11)$$

Note that if $p_i^2 = p_j^2 = 0$ we have the identity

$$K_{ij}^\wedge K_{ij}^\vee = -\frac{1}{2} p_i^+ p_j^+ (p_i + p_j)^2 \quad \text{for } p_i^2 = p_j^2 = 0 \quad (12)$$

With only one leg off-shell we can always write the denominators in terms of on-shell momenta and exploit this identity. For example if only leg 4 is off-shell we have

$$A_{tree}^{\wedge\wedge\wedge\vee} = \frac{1}{2} \left[\frac{p_4^+ K_{14}^\wedge}{p_1^+ K_{32}^\vee} + \frac{p_4^+ K_{43}^\wedge}{p_3^+ K_{21}^\vee} \right] = \frac{p_4^+}{2K_{32}^\vee K_{21}^\vee} \sum_i \frac{K_{4i}^\wedge K_{i2}^\vee}{p_i^+} = -\frac{p_4^+ p_2^+ p_4^2}{4K_{32}^\vee K_{21}^\vee} \quad \text{for } p_1^2 = p_2^2 = p_3^2 = 0 \quad (13)$$

which, of course, vanishes on-shell. Corresponding expressions when other legs are off shell are obtained by always writing the denominators so they involve the on shell legs only. We obtain

$$A_{tree}^{\wedge\wedge\wedge\vee} = -\frac{p_4^{+2} p_1^+ p_3^2}{4p_3^+ K_{14}^\vee K_{21}^\vee} \quad \text{for } p_1^2 = p_2^2 = p_4^2 = 0 \quad (14)$$

$$A_{tree}^{\wedge\wedge\wedge\vee} = -\frac{p_4^{+2} p_3^+ p_1^2}{4p_1^+ K_{32}^\vee K_{43}^\vee} \quad \text{for } p_2^2 = p_3^2 = p_4^2 = 0 \quad (15)$$

$$A_{tree}^{\wedge\wedge\wedge\vee} = -\frac{p_4^{+3} p_2^2}{4p_2^+ K_{14}^\vee K_{43}^\vee} \quad \text{for } p_1^2 = p_3^2 = p_4^2 = 0 \quad (16)$$

Thus the on-shell amplitudes for all like helicities and all but one like helicities vanish, a well-known result which applies to the scattering of any number of gluons.

For the case with all four gluons off-shell, the denominators can't be factored so simply, but we can still get a reasonably compact result.

$$A_{tree}^{\wedge\wedge\wedge\vee} = -\frac{p_4^+ (K_{43}^\wedge K_{32}^\vee p_2^2 + K_{14}^\wedge K_{43}^\vee p_2^2 + K_{21}^\wedge K_{14}^\vee p_3^2 + K_{32}^\wedge K_{21}^\vee p_4^2)}{p_1^+ p_2^+ p_3^+ (p_1 + p_2)^2 (p_2 + p_3)^2} \quad (17)$$

The only non-zero four point trees are those with two of each helicity. The diagrams with adjacent like helicity are shown in Fig. 3. Applying the light-cone gauge rules to these diagrams gives

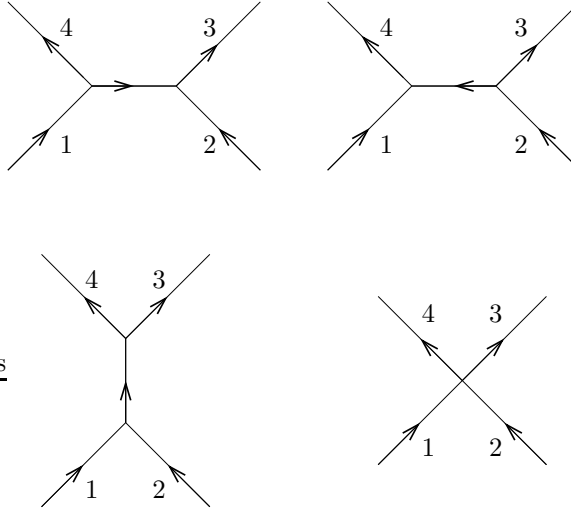


Figure 3: Tree diagrams for the gluon scattering with polarizations $\wedge\wedge\vee\vee$.

$$\begin{aligned}
A_{tree}^{\wedge\wedge\vee\vee} &= -\frac{1}{(p_1^+ + p_4^+)^2} \left[\frac{p_1^+ p_3^+}{p_2^+ p_4^+} \frac{K_{14}^\wedge K_{32}^\vee}{(p_1 + p_4)^2} + \frac{p_2^+ p_4^+}{p_1^+ p_3^+} \frac{K_{14}^\wedge K_{32}^\vee}{(p_1 + p_4)^2} + \frac{p_1^+ p_3^+ + p_2^+ p_4^+}{2} \right] \\
&\quad - \frac{(p_1^+ + p_2^+)^2 K_{21}^\wedge K_{43}^\vee}{p_1^+ p_2^+ p_3^+ p_4^+ (p_1 + p_2)^2}
\end{aligned} \tag{18}$$

With all legs on shell the right side can be dramatically simplified. We shall need some further identities:

$$\begin{aligned}
K_{14}^\wedge K_{32}^\vee + K_{14}^\vee K_{32}^\wedge &= -\frac{p_1^+ p_3^+ + p_2^+ p_4^+}{2} (p_1 + p_4)^2 + \frac{(p_1^+ + p_4^+)^2}{2} (p_1 + p_2)^2 \\
&\quad + \frac{p_1^+ + p_4^+}{2} [p_1^+ p_3^+ (p_1^* - p_3^*) + p_2^+ p_4^+ (p_4^* - p_2^*)] \\
&\rightarrow -\frac{p_1^+ p_3^+ + p_2^+ p_4^+}{2} (p_1 + p_4)^2 + \frac{(p_1^+ + p_4^+)^2}{2} (p_1 + p_2)^2 \quad (\text{On Shell})
\end{aligned} \tag{19}$$

Here, when some legs are off-shell, we use the shorthand notation $p_i^* \equiv p_i^2/p_i^+$ to simplify the writing.

$$\begin{aligned}
p_2^+ p_4^+ K_{14}^\wedge K_{32}^\vee - p_1^+ p_3^+ K_{14}^\vee K_{32}^\wedge &= -(p_1^+ + p_4^+)^2 K_{21}^\wedge K_{43}^\vee + (p_1^+ + p_4^+) (p_1^+ K_{32}^\wedge K_{43}^\vee - p_3^+ K_{21}^\wedge K_{14}^\vee) \\
&= -(p_1^+ + p_4^+)^2 K_{21}^\wedge K_{43}^\vee \\
&\quad + \frac{(p_1^+ + p_4^+)}{(p_1^+ + p_2^+)} (p_1^+ p_2^+ K_{43}^\wedge K_{43}^\vee - 2p_1^+ p_3^+ K_{21}^\wedge K_{43}^\vee + p_3^+ p_4^+ K_{21}^\wedge K_{21}^\vee) \\
&= -\frac{p_1^+ + p_4^+}{p_1^+ + p_2^+} [(p_1^+ p_3^+ + p_2^+ p_4^+) K_{21}^\wedge K_{43}^\vee - p_1^+ p_2^+ K_{43}^\wedge K_{43}^\vee - p_3^+ p_4^+ K_{21}^\wedge K_{21}^\vee] \\
&= -\frac{p_1^+ + p_4^+}{p_1^+ + p_2^+} \left[(p_1^+ p_3^+ + p_2^+ p_4^+) K_{21}^\wedge K_{43}^\vee + p_1^+ p_2^+ p_3^+ p_4^+ \left((p_1 + p_2)^2 - \frac{1}{2} (p_1^+ + p_2^+) (p_1^* + p_2^* - p_3^* - p_4^*) \right) \right] \\
&\rightarrow -\frac{p_1^+ + p_4^+}{p_1^+ + p_2^+} [(p_1^+ p_3^+ + p_2^+ p_4^+) K_{21}^\wedge K_{43}^\vee + p_1^+ p_2^+ p_3^+ p_4^+ (p_1 + p_2)^2] \quad (\text{On Shell}) \tag{20}
\end{aligned}$$

We use these identities to manipulate the first line to a form which shows no singularity at $p_1^+ + p_4^+ = 0$ when all legs are on-shell:

$$\begin{aligned}
A_{tree}^{\wedge\wedge\vee\vee} &= \frac{(p_1 + p_2)^2}{2(p_1 + p_4)^2} - \frac{K_{21}^\wedge K_{43}^\vee [(p_1^+ + p_2^+)^2 (p_1 + p_4)^2 - (p_1^+ p_3^+ + p_2^+ p_4^+) (p_1 + p_2)^2]}{p_1^+ p_2^+ p_3^+ p_4^+ (p_1 + p_2)^2 (p_1 + p_4)^2} \\
&\quad - \frac{p_2^+ p_4^+ (p_1^* - p_3^*) + p_1^+ p_3^+ (p_4^* - p_2^*)}{2(p_1^+ + p_4^+) (p_1 + p_4)^2}
\end{aligned} \tag{21}$$

The quantity in square brackets in the numerator of the second term can be related to

$$\begin{aligned}
2(K_{21}^\wedge K_{43}^\vee + K_{21}^\vee K_{43}^\wedge) &= -(p_1^+ p_3^+ + p_2^+ p_4^+) (p_1 + p_2)^2 + (p_1^+ + p_2^+)^2 (p_1 + p_4)^2 \\
&\quad + (p_1^+ + p_2^+) [p_1^+ p_3^+ (p_1^* - p_3^*) + p_2^+ p_4^+ (p_2^* - p_4^*)]
\end{aligned} \tag{22}$$

so it easily follows that

$$\begin{aligned}
A_{tree}^{\wedge\wedge\vee\vee} &= \frac{(p_1 + p_2)^2}{2(p_1 + p_4)^2} - \frac{2(K_{21}^\wedge K_{43}^\vee + K_{21}^\vee K_{43}^\wedge) (p_1^+ + p_2^+)^2 (p_1 + p_4)^2}{p_1^+ p_2^+ p_3^+ p_4^+ (p_1 + p_2)^2 (p_1 + p_4)^2} - \frac{p_2^+ p_4^+ (p_1^* - p_3^*) + p_1^+ p_3^+ (p_4^* - p_2^*)}{2(p_1^+ + p_4^+) (p_1 + p_4)^2} \\
&\quad + \frac{K_{21}^\wedge K_{43}^\vee (p_1^+ + p_2^+) [p_1^+ p_3^+ (p_1^* - p_3^*) + p_2^+ p_4^+ (p_2^* - p_4^*)]}{p_1^+ p_2^+ p_3^+ p_4^+ (p_1 + p_2)^2 (p_1 + p_4)^2} \\
&= -\frac{2K_{21}^\wedge K_{43}^\vee}{p_1^+ p_2^+ p_3^+ p_4^+ (p_1 + p_2)^2 (p_1 + p_4)^2}
\end{aligned} \tag{23}$$

$$+ \frac{(p_1^+ + p_2^+)(p_1^* + p_2^* - p_3^* - p_4^*)}{2(p_1 + p_4)^2} - \frac{p_2^+ p_4^+ (p_1^* - p_3^*) + p_1^+ p_3^+ (p_4^* - p_2^*)}{2(p_1^+ + p_4^+)(p_1 + p_4)^2} \quad (24)$$

$$+ \frac{(p_1^+ + p_2^+)^2 (p_1^* + p_2^*)(p_3^* + p_4^*)}{2(p_1 + p_2)^2 (p_1 + p_4)^2} + \frac{K_{21}^\wedge K_{43}^\vee (p_1^+ + p_2^+) [p_1^+ p_3^+ (p_1^* - p_3^*) + p_2^+ p_4^+ (p_2^* - p_4^*)]}{p_1^+ p_2^+ p_3^+ p_4^+ (p_1 + p_2)^2 (p_1 + p_4)^2} \quad (25)$$

$$\rightarrow - \frac{2 K_{21}^\wedge K_{43}^\vee 2}{p_1^+ p_2^+ p_3^+ p_4^+ (p_1 + p_2)^2 (p_1 + p_4)^2} \quad (\text{On Shell}) \quad (25)$$

$$= \frac{p_3^+ p_4^+ K_{12}^\wedge 4}{2 p_1^+ p_2^+ K_{12}^\wedge K_{23}^\wedge K_{34}^\wedge K_{41}^\wedge} \quad (26)$$

which is essentially the Parke-Taylor form of the answer. The bispinor matrix elements employed by them differ from our K_{ij} by factors of p^+ .

The other distinct helicity arrangement for four gluon scattering is shown in Fig. 4. The light-cone gauge rules for these diagrams give

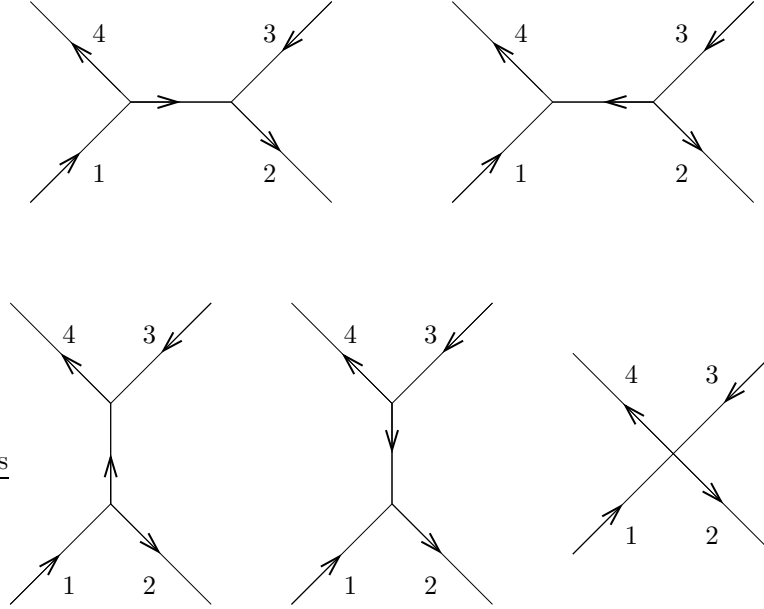


Figure 4: Tree diagrams for gluon scattering with alternating helicity, $\wedge \vee \wedge \vee$

$$A_{tree}^{\wedge \vee \wedge \vee} = - \frac{1}{(p_1^+ + p_4^+)^2} \left[\frac{p_1^+ p_2^+}{p_3^+ p_4^+} \frac{K_{14}^\vee K_{32}^\wedge}{(p_1 + p_4)^2} + \frac{p_3^+ p_4^+}{p_1^+ p_2^+} \frac{K_{14}^\wedge K_{32}^\vee}{(p_1 + p_4)^2} - \frac{p_1^+ p_2^+ + p_3^+ p_4^+}{2} \right] \\ - \frac{1}{(p_1^+ + p_2^+)^2} \left[\frac{p_1^+ p_4^+}{p_2^+ p_3^+} \frac{K_{43}^\wedge K_{21}^\vee}{(p_1 + p_2)^2} + \frac{p_2^+ p_3^+}{p_1^+ p_4^+} \frac{K_{43}^\vee K_{21}^\wedge}{(p_1 + p_2)^2} - \frac{p_1^+ p_4^+ + p_2^+ p_3^+}{2} \right] \quad (27)$$

where the quartic vertex contribution has been split between the last terms in each of the square brackets. Notice that the second line on the right side is obtained from the first line with the relabeling substitutions $1 \rightarrow 2 \rightarrow 3 \rightarrow 4 \rightarrow 1$ and $\wedge \rightarrow \vee \rightarrow \wedge$. Furthermore the first line can be obtained from the first line on the right of (18) by interchanging $2 \leftrightarrow 3$ and multiplying by the factor -1 . Thus by inspection we immediately obtain the simplifications

$$A_{tree}^{\wedge \vee \wedge \vee} = - \frac{p_{13}^2}{2 p_{14}^2} - \frac{(p_1^+ p_2^+ + p_3^+ p_4^+) K_{31}^\wedge K_{42}^\vee}{p_1^+ p_2^+ p_3^+ p_4^+ p_{14}^2} - \frac{p_{13}^2}{2 p_{12}^2} - \frac{(p_2^+ p_3^+ + p_1^+ p_4^+) K_{13}^\wedge K_{42}^\vee}{p_1^+ p_2^+ p_3^+ p_4^+ p_{12}^2}$$

$$\begin{aligned}
& + \frac{p_3^+ p_4^+ (p_1^* - p_2^*) + p_1^+ p_2^+ (p_4^* - p_3^*)}{2p_{14}^2 p_{14}^+} + \frac{p_1^+ p_4^+ (p_2^* - p_3^*) + p_2^+ p_3^+ (p_1^* - p_4^*)}{2p_{12}^2 p_{12}^+} \\
= & - \frac{p_{13}^2 (p_{12}^2 + p_{14}^2)}{2p_{14}^2 p_{12}^2} - \frac{2K_{31}^\wedge K_{42}^\vee [K_{31}^\wedge K_{42}^\vee + K_{31}^\vee K_{42}^\wedge]}{p_1^+ p_2^+ p_3^+ p_4^+ p_{14}^2 p_{12}^2} \\
& - K_{31}^\wedge K_{42}^\vee \frac{p_3^+ p_4^+ (p_1^2 + p_2^2) + p_1^+ p_2^+ (p_3^2 + p_4^2) - p_2^+ p_3^+ (p_1^2 + p_4^2) - p_1^+ p_4^+ (p_2^2 + p_3^2)}{p_1^+ p_2^+ p_3^+ p_4^+ p_{14}^2 p_{12}^2} \\
& + \frac{p_3^+ p_4^+ (p_1^* - p_2^*) + p_1^+ p_2^+ (p_4^* - p_3^*)}{2p_{14}^2 p_{14}^+} + \frac{p_1^+ p_4^+ (p_2^* - p_3^*) + p_2^+ p_3^+ (p_1^* - p_4^*)}{2p_{12}^2 p_{12}^+} \\
= & - \frac{2K_{31}^{\wedge 2} K_{42}^{\vee 2}}{p_1^+ p_2^+ p_3^+ p_4^+ p_{12}^2 p_{14}^2} - \frac{p_{13}^+ p_{24}^+ (p_1^* + p_3^*) (p_2^* + p_4^*)}{2p_{12}^2 p_{14}^2} + \frac{p_{13}^2 [p_4^+ p_2^* + p_2^+ p_4^* + p_3^+ p_1^* + p_1^+ p_3^*]}{2p_{12}^2 p_{14}^2} \\
& - K_{31}^\wedge K_{42}^\vee \frac{p_3^+ p_4^+ (p_1^2 + p_2^2) + p_1^+ p_2^+ (p_3^2 + p_4^2) - p_2^+ p_3^+ (p_1^2 + p_4^2) - p_1^+ p_4^+ (p_2^2 + p_3^2)}{p_1^+ p_2^+ p_3^+ p_4^+ p_{14}^2 p_{12}^2} \\
& + \frac{p_3^+ p_4^+ (p_1^* - p_2^*) + p_1^+ p_2^+ (p_4^* - p_3^*)}{2p_{14}^2 p_{14}^+} + \frac{p_1^+ p_4^+ (p_2^* - p_3^*) + p_2^+ p_3^+ (p_1^* - p_4^*)}{2p_{12}^2 p_{12}^+} \\
\rightarrow & - \frac{2K_{31}^{\wedge 2} K_{42}^{\vee 2}}{p_1^+ p_2^+ p_3^+ p_4^+ p_{12}^2 p_{14}^2}, \quad (\text{On Shell}) \tag{28} \\
= & \frac{p_2^+ p_4^+ K_{13}^{\wedge 4}}{2p_1^+ p_3^+ K_{12}^\wedge K_{23}^\wedge K_{34}^\wedge K_{41}^\wedge} \tag{29}
\end{aligned}$$

where we have used the shorthand notation $p_{ij} = p_i + p_j$. Again we note the characteristic Parke-Taylor form in the last line.

5 Gluon Self-Energy

In order to acquaint the reader with some of the novelties of calculations using the δ regulator of ultraviolet divergences, we calculate the gluon self-energy diagrams in complete detail, with an explicit separation of all divergences and Lorentz-violating artifacts. Recall that the choice of light-cone gauge has sacrificed manifest Lorentz invariance, leaving only the light-cone Galilei subgroup of the Poincaré group as a manifest symmetry. In addition, discretization of p^+ provides an infrared regulator that breaks the Lorentz symmetry generated by M^{+-} , under which p^+ and p^- scale oppositely. Another novelty in the calculation comes from our use of dual momentum variables: for an N point amplitude there are N independent dual momenta but only $N - 1$ independent actual momenta (because of momentum conservation). In the bare Feynman rules this redundancy is taken care of by a new symmetry under the translation of all dual momenta by the same amount. The δ regulator inserts a factor $e^{-\delta \sum \mathbf{q}_i^2}$, where \mathbf{q}_i are the dual momenta assigned to the loops. With $\delta > 0$ the dual momentum translation invariance is explicitly broken, and so is the Galilei boost part of the residual light-cone Galilei invariance. The upshot of all this [4] is that in the presence of nonzero δ and discrete p^+ , manifest Poincaré invariance is broken to translation invariance in the + and transverse directions and the $O(2)$ rotation invariance in the transverse plane, as well as the conservation of discrete p^+ . We demand that the full Poincaré symmetry is restored as $\delta \rightarrow 0$ and p^+ becomes continuous, and we shall determine the counterterms necessary to achieve this to one-loop order.

We call the bare gluon self-energy Π^{ij} , and stress that it includes contributions arising from the elimination of the gauge field components A^\pm from the formalism. We continue to use the helicity basis for the gluon polarization 1, 2: $\wedge = (1 + i2)/\sqrt{2}$, $\vee = (1 - i2)/\sqrt{2}$. It is convenient to introduce the Schwinger representation for each internal propagator

$$\frac{e^{-\delta \mathbf{q}^2}}{(q - k_0)^2 (q - k_1)^2} = \int dT_1 dT_2 e^{-T_1 (q - k_0)^2 - T_2 (q - k_1)^2 - \delta \mathbf{q}^2} \tag{30}$$

where we have used dual momenta k_0, k_1 with the momentum carried by the propagator $p = k_1 - k_0$, and we take $k_0^+ = 0$. The standard light-cone evaluation of the q^- integration using the calculus of residues is equivalent to the insertion $\pi\delta((T_1 + T_2)q^+ - T_2 p^+)$ in the integral over the remaining components of momentum. The integral over transverse momentum is easily done by completing the square in the exponent. We leave $q^+ = lm$, $l = 1, 2, \dots, M = p^+/m$, discretized to regulate the $q^+ = 0$ singularities. First consider

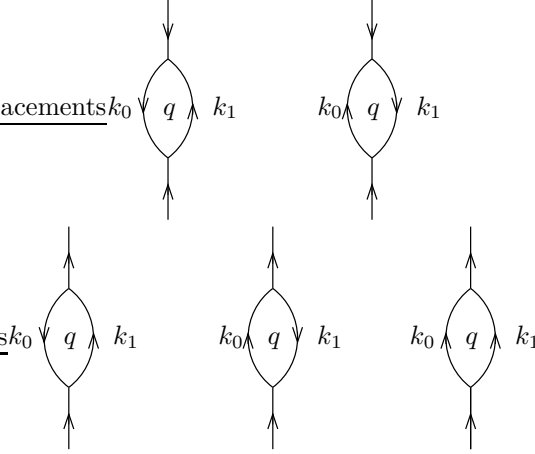


Figure 5: The self energy diagrams for $\Pi^{\wedge\wedge}$ (top line) and $\Pi^{\wedge\vee}$ (bottom line).

the like helicity component $\Pi^{\wedge\wedge}$.

$$\begin{aligned} \Pi^{\wedge\wedge} &= \frac{g^2 N_c}{2\pi^2} \int_0^\infty dT \int_0^1 dx \frac{\delta^2 [xk_0^\vee + (1-x)k_1^\vee]^2}{(T+\delta)^3} \\ &\quad \exp \left\{ -Tx(1-x)p^2 - \frac{\delta T}{T+\delta} (x\mathbf{k}_0 + (1-x)\mathbf{k}_1)^2 \right\} \end{aligned} \quad (31)$$

$$\rightarrow \frac{g^2 N_c}{4\pi^2} \int_0^1 dx [xk_0^\wedge + (1-x)k_1^\wedge]^2 = \frac{g^2 N_c}{12\pi^2} [k_0^{\wedge 2} + k_1^{\wedge 2} + k_0^\wedge k_1^\wedge] \quad (32)$$

where we have included the factor of N_c arising from our substitution rule giving the color dependence of the large N_c limit. In this expression, it was safe to take q^+ continuous since there are no $q^+ = 0$ singularities in the integrand. We have also changed variables from Schwinger parameters to $T = T_1 + T_2$, $x = T_1/(T_1 + T_2)$. Lorentz invariance would imply that $\Pi^{\wedge\wedge} = 0$ on-shell, otherwise a single isolated gluon could flip its helicity. Indeed, the Galilei boost invariance alone would imply that it vanishes. But the δ regulator breaks this invariance. We see by inspection that the whole T integration region a finite distance away from the origin vanishes as $\delta \rightarrow 0$, but the region with $T = O(\delta)$ survives the limit due to the $(T+\delta)^{-3}$ behavior of the integrand. The result is nevertheless finite and a quadratic polynomial in the dual momenta. Note that in addition to violating Lorentz invariance the result also violates the dual momentum translation symmetry. We therefore must introduce a counterterm that exactly cancels this result:

$$\Pi_{\text{TOT}}^{\wedge\wedge} \equiv \Pi^{\wedge\wedge} + \Pi_{\text{C.T.}}^{\wedge\wedge} = 0. \quad (33)$$

We now briefly discuss how this counterterm is incorporated in the worldsheet description. The dual momenta $\mathbf{k}_0, \mathbf{k}_1$ are the boundary values of the worldsheet field $\mathbf{q}(\sigma, \tau)$. We can write the contribution of the counterterm to the worldsheet path integral as

$$\frac{-T}{2p^+} \Pi_{\text{C.T.}}^{\wedge\wedge} = \frac{T}{2p^+} \frac{g^2 N_c}{12\pi^2} \left[\frac{3}{2} k_0^{\wedge 2} + \frac{3}{2} k_1^{\wedge 2} - \frac{1}{2} p^{\wedge 2} \right]$$

$$= \frac{g^2 N_c}{16\pi^2} \int d\tau \frac{q^\wedge(0) + q^\wedge(p^+)}{p^+} - \frac{g^2 N_c}{48\pi^2} \int d\tau d\sigma \left(\frac{\partial q^\wedge}{\partial \sigma} \right)^2 \quad (34)$$

We see that the counter term can be associated with new terms in the worldsheet action, in a fashion similar to that in [4]. The first term is a boundary term and the second is a bulk term. In order to ensure that the term enters only for like helicities, additional factors of Grassmann variables $\bar{S}^\vee(\sigma)S^\vee(\sigma)$ must also be included (see [5]).

Next we turn to the helicity conserving contributions to Π .

$$\begin{aligned} \Pi^{\wedge\vee} &= \Pi^{\vee\wedge} = \frac{g^2 N_c}{4\pi^2} \sum_{q^+} \int_0^\infty dT \int_0^1 dx \delta(q^+ - (1-x)p^+) \left[\frac{1}{(T+\delta)^2} + \frac{\delta^2[x\mathbf{k}_0 + (1-x)\mathbf{k}_1]^2}{(T+\delta)^3} \right] \\ &\quad \left(1 + \frac{1}{x} + \frac{1}{(1-x)^2} \right) \exp \left\{ -Tx(1-x)p^2 - \delta T \frac{(x\mathbf{k}_0 + (1-x)\mathbf{k}_1)^2}{(T+\delta)} \right\} \\ &= \frac{g^2 N_c}{4\pi^2} \frac{1}{p^+} \sum_{0 < q^+ < p^+} \int_0^\infty dT \left[\frac{1}{(T+\delta)^2} + \frac{\delta^2[x\mathbf{k}_0 + (1-x)\mathbf{k}_1]^2}{(T+\delta)^3} \right] \\ &\quad \left(1 + \frac{1}{x^2} + \frac{1}{(1-x)^2} \right) \exp \left\{ -Tx(1-x)p^2 - \frac{\delta T}{T+\delta} (x\mathbf{k}_0 + (1-x)\mathbf{k}_1)^2 \right\} \Big|_{x=1-q^+/p^+} \end{aligned} \quad (35)$$

The quadratic divergence in $\Pi^{\wedge\vee}$ can be simply extracted with an integration by parts. We observe that

$$\begin{aligned} \left[\frac{1}{(T+\delta)^2} + \frac{\delta^2[x\mathbf{k}_0 + (1-x)\mathbf{k}_1]^2}{(T+\delta)^3} \right] \exp \left\{ -\frac{\delta T}{T+\delta} (x\mathbf{k}_0 + (1-x)\mathbf{k}_1)^2 \right\} &= \\ -\frac{\partial}{\partial T} \frac{1}{T+\delta} \exp \left\{ -\frac{\delta T}{T+\delta} (x\mathbf{k}_0 + (1-x)\mathbf{k}_1)^2 \right\} \end{aligned} \quad (36)$$

So we can rewrite the self energy as

$$\begin{aligned} \Pi^{\wedge\vee} &= -\frac{g^2 N_c}{4\pi^2} p^2 \sum_{q^+} \frac{1}{p^+} \left(\frac{q^+(p^+ - q^+)}{p^{+2}} + \frac{p^+ - q^+}{q^+} + \frac{q^+}{p^+ - q^+} \right) I(H\delta) \\ &\quad + \frac{g^2 N_c}{4\pi^2} \frac{1}{\delta} \sum_{q^+} \frac{1}{p^+} \left(1 + \frac{p^{+2}}{q^{+2}} + \frac{p^{+2}}{(p^+ - q^+)^2} \right) \end{aligned} \quad (37)$$

$$H \equiv x(1-x)p^2, \quad x = 1 - \frac{q^+}{p^+} \quad (38)$$

$$I(H\delta) \equiv \int_0^\infty \frac{e^{-H\delta u - \delta u(x\mathbf{k}_0 + (1-x)\mathbf{k}_1)^2/(1+u)}}{1+u} \underset{\delta \rightarrow 0}{\sim} -\gamma - \ln\{H\delta\} \quad (39)$$

where $\gamma = -\Gamma'(1)/\Gamma(1)$ is Euler's constant. Note that the dual momentum translation invariance is restored in this quantity as $\delta \rightarrow 0$, apparently for accidental reasons. Clearly the q^+ sums diverge when q^+ becomes continuous. These divergences are spurious artifacts of the light-cone gauge and have nothing to do with the usual ultraviolet divergences of the gauge theory. They must cancel in physical quantities without invoking renormalization or counterterms. In our approach the q^+ sum just corresponds to integration over the location on the worldsheet of the boundary representing the loop. On the worldsheet lattice this location is an integer l with $x = l/M$ and M is the discretized total plus momentum entering the self energy: $p^+ = mM$. In the above formulas, \sum_{q^+} means $m \sum_{l=1}^{M-1}$. The discreteness of p^+ regulates the endpoint x integral divergences.

Let us discuss first the fate of the quadratic $1/\delta$ divergence, which for discrete p^+ reads, with $q^+ = lm$:

$$\frac{g^2 N_c}{4\pi^2} \frac{1}{M\delta} \sum_{l=1}^{M-1} \left(1 + \frac{M^2}{l^2} + \frac{M^2}{(M-l)^2} \right) \sim \frac{g^2 N_c}{4\pi^2} \frac{1}{\delta} \left(\frac{\pi^2}{3} M - 1 + O\left(\frac{1}{M}\right) \right) \quad (40)$$

where the right side indicates the large M behavior of the sums. The term linear in $M = p^+/m$ cannot be canceled by a gluon self mass, because it is linear in p^+ . However, precisely because it is linear in p^+ , it represents a constant $-g^2 N_c M / (24p^+ \delta) = -g^2 N_c / (24m\delta)$ added to the energy $p^- = \mathbf{p}^2 / 2p^+$ of each gluon. Of course the number of gluons is not fixed as a function of time so we can't say that this constant is unobservable. If there are n gluons present at a given time, a constant e_0 added to each gluon energy would add ne_0 to the total energy. In the worldsheet picture the number of gluons changes whenever an internal boundary terminates or a new one originates. And the contribution of each gluon to the worldsheet action would be $-e_0 t$ where t is the time the gluon exists. Thus a constant added to p^- can be interpreted as energy associated with the boundary of the worldsheet representing that gluon. The corresponding contribution to the worldsheet action is then $-e_0 L/2$ where L is the sum of all the lengths of all the boundaries in the worldsheet. (Note that an internal boundary representing a loop has total length $2T$ where T is the time the boundary exists.) In other words $e_0/2$ contributes like a boundary cosmological constant. If we start with a nonzero boundary cosmological constant λ_b in zeroth order, we can tune its value to cancel the linear terms in p^+ generated by loop effects. Its lowest order value is then

$$\lambda_b = +\frac{g^2 N_c}{48m\delta} \quad (41)$$

After this cancellation, there is left behind a constant which can be canceled by a gluon mass counterterm $\delta\mu^2$. So to this order

$$\delta\mu^2 = \frac{g^2 N_c}{4\pi^2 \delta} \quad (42)$$

Of course, the gluon mass is zero in tree approximation, but since loop corrections generate a gluon mass, the tree value must be non-zero and adjusted to cancel the loop contributions order by order in perturbation theory. A nonzero mass at tree level violates gauge invariance, which means a violation of Lorentz invariance in the completely fixed lightcone gauge. So an alternative prescription is: in lightcone gauge, allow a nonzero gluon mass μ_0^2 as an input parameter, and calculate physical quantities as functions of this parameter. Finally, choose a value of this parameter that restores Lorentz invariance. Note that to one loop, $\mu^2 = 0$ requires a tachyonic gluon mass: $\mu_0^2 = -\delta\mu^2$. A gluon mass is introduced into the worldsheet formalism for gauge theory exactly as in the scalar case [4].

Next we turn to the logarithmic divergences in the self energy. Call $p = q' - q$ and remember that $x = q^+/p^+$. Including the above mentioned counterterms, we then find

$$\begin{aligned} \Pi_{\text{TOT}}^{\wedge\vee} &= \Pi^{\wedge\vee} - 2p^+ \lambda_b + \delta\mu^2 \\ &= \frac{g^2 N_c}{4\pi^2} p^2 \sum_{q^+} \left(\frac{x(1-x)-2}{p^+} + \frac{1}{q^+} + \frac{1}{p^+ - q^+} \right) \ln \{x(1-x)p^2\delta e^\gamma\} \end{aligned} \quad (43)$$

$$\sim \frac{g^2 N_c}{4\pi^2} p^2 \left(\sum_{q^+} \left[\frac{1}{q^+} + \frac{1}{p^+ - q^+} \right] \ln \left\{ \frac{q^+(p^+ - q^+)}{p^{+2}} p^2 \delta e^\gamma \right\} - \frac{11}{6} \ln(p^2 \delta e^\gamma) + \frac{67}{18} \right) \quad (44)$$

Note that this quantity is negative by virtue of the (divergent) q^+ sums, in accordance with the requirements of unitarity. The divergent p^+ dependent coefficient of $\ln \delta$ is characteristic of light-cone gauge. We shall find that these unusual terms cancel against corresponding terms coming from triangle and box diagrams. To simplify future equations, we give the anomalous quantity in parentheses a name:

$$\mathcal{A}(p^2, p^+) \equiv \sum_{q^+} \left[\frac{1}{q^+} + \frac{1}{p^+ - q^+} \right] \ln \{x(1-x)p^2\delta e^\gamma\}. \quad (45)$$

We shall find this quantity occurring in vertex calculations. Then to summarize this section:

$$\Pi_{\text{TOT}}^{\wedge\vee} = \frac{g^2 N_c}{4\pi^2} p^2 \left[\mathcal{A}(p^2, p^+) - \frac{11}{6} \ln(p^2 \delta e^\gamma) + \frac{67}{18} \right] \quad (46)$$

$$\Pi_{\text{TOT}}^{\wedge\wedge} = \Pi_{\text{TOT}}^{\vee\vee} = 0 \quad (47)$$

6 Cubic Vertex Function

We shall not include calculational details for the one loop corrections to the cubic vertex function. They can be found in [14]. Instead we present the final answers for the vertex corrections with two on-shell gluons.

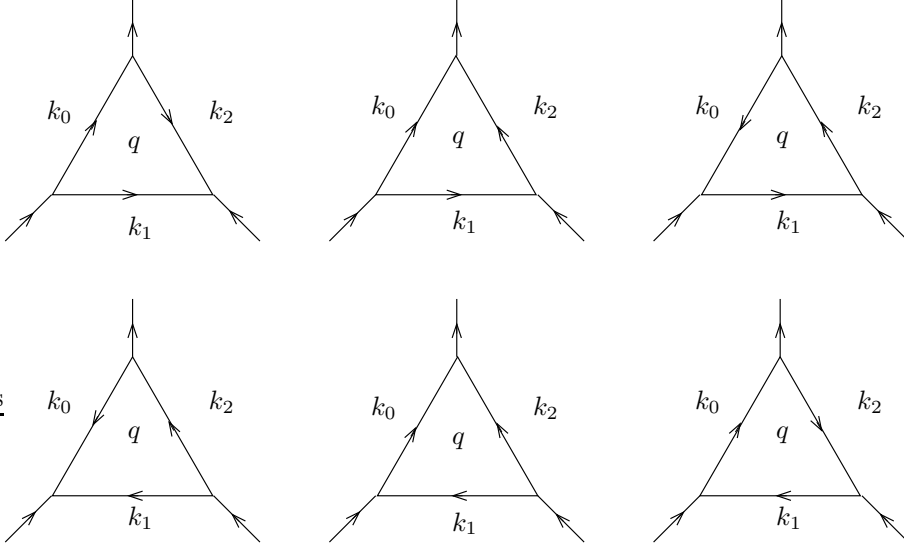


Figure 6: The triangle diagrams contributing to $\Gamma^{\wedge\wedge\vee}$.

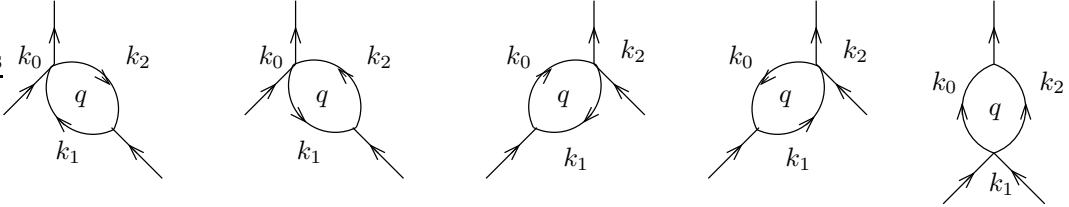


Figure 7: The swordfish diagrams contributing to $\Gamma^{\wedge\wedge\vee}$.

We put the combination of swordfish and triangle diagrams (see Figs. 6,7) with two like-helicities and two legs on-shell in the form

$$\Gamma_{1 \text{ loop}} = -\frac{(g\sqrt{N_c})^3}{12\pi^2} \sum_i k_i - \frac{g^2 N_c}{8\pi^2} \Gamma_{\text{tree}} \left(\frac{70}{9} - \frac{11}{3} \ln(\delta p_o^2 e^\gamma) + S \right) + \alpha \frac{(g\sqrt{N_c})^3}{12\pi^2} \frac{K}{p_o^+} \quad (48)$$

where the vectors k_i, K carry the polarization of the two like- helicity gluons, p_o is the four-momentum of the off-shell gluon, $\alpha = 1$ when the on-shell gluons have like-helicity, and $\alpha = 0$ otherwise. Finally S is an infrared sensitive term that depends on the location of the off-shell gluon, but not on any of the gluon helicities. In the case $p_1^+, p_2^+ > 0$, we denote by $S_i^{q^+}(p_1, p_2)$ the value of S when leg i is off-shell, and with loop momentum chosen so that q^+ is the longitudinal momentum of the internal line joining leg 1 to leg 3, satisfying $0 < q^+ < p_{12}^+$. Then,

$$S_1^{q^+}(p_1, p_2) = \sum_{q^+ < p_1^+} \left\{ \left[\frac{2}{q^+} + \frac{1}{p_1^+ + p_2^+ - q^+} + \frac{1}{p_1^+ - q^+} \right] \left(\ln(\delta p_1^2 e^\gamma) + \ln \frac{q^+}{p_1^+} \right) \right.$$

$$\begin{aligned}
& + \left[\frac{2}{p_1^+ - q^+} - \frac{1}{p_1^+ + p_2^+ - q^+} + \frac{1}{q^+} \right] \ln \frac{p_1^+ - q^+}{p_1^+} \} \\
& + \sum_{q^+ > p_1^+} \left\{ \left[\frac{1}{q^+} + \frac{2}{p_1^+ + p_2^+ - q^+} + \frac{1}{q^+ - p_1^+} \right] \left(\ln(\delta p_1^2 e^\gamma) + \ln \frac{p_1^+ + p_2^+ - q^+}{p_2^+} \right) \right. \\
& \left. + \sum_{q^+ \neq p_1^+} \left[\frac{1}{q^+} + \frac{2}{p_1^+ + p_2^+ - q^+} + \frac{1}{q^+ - p_1^+} \right] \ln \frac{p_1^+ + p_2^+ - q^+}{p_1^+ + p_2^+} \right\} \tag{49}
\end{aligned}$$

$$\begin{aligned}
S_2^{q^+}(p_1, p_2) = & \sum_{q^+ \neq p_1^+} \left[\frac{2}{q^+} + \frac{1}{p_1^+ + p_2^+ - q^+} + \frac{1}{p_1^+ - q^+} \right] \ln \frac{q^+}{p_1^+ + p_2^+} \\
& + \sum_{q^+ < p_1^+} \left\{ \left[\frac{2}{q^+} + \frac{1}{p_1^+ + p_2^+ - q^+} + \frac{1}{p_1^+ - q^+} \right] \left(\ln(\delta p_2^2 e^\gamma) + \ln \frac{q^+}{p_1^+} \right) \right\} \\
& + \sum_{q^+ > p_1^+} \left\{ \left[\frac{1}{q^+} + \frac{2}{p_1^+ + p_2^+ - q^+} + \frac{1}{q^+ - p_1^+} \right] \left(\ln(\delta p_2^2 e^\gamma) + \ln \frac{p_1^+ + p_2^+ - q^+}{p_2^+} \right) \right. \\
& \left. + \left[\frac{2}{q^+ - p_1^+} + \frac{1}{p_1^+ + p_2^+ - q^+} - \frac{1}{q^+} \right] \ln \frac{q^+ - p_1^+}{p_2^+} \right\} \tag{50}
\end{aligned}$$

$$\begin{aligned}
S_3^{q^+}(p_1, p_2) = & \sum_{q^+ < p_1^+} \left\{ \left[\frac{2}{q^+} + \frac{1}{p_1^+ + p_2^+ - q^+} + \frac{1}{p_1^+ - q^+} \right] \left(\ln(\delta p_{12}^2 e^\gamma) + \ln \frac{q^+}{p_1^+ + p_2^+} \right) \right. \\
& + \left[\frac{1}{q^+} + \frac{2}{p_1^+ + p_2^+ - q^+} + \frac{1}{q^+ - p_1^+} \right] \ln \frac{p_1^+ + p_2^+ - q^+}{p_1^+ + p_2^+} \\
& + \left[\frac{2}{p_1^+ - q^+} - \frac{1}{p_1^+ + p_2^+ - q^+} + \frac{1}{q^+} \right] \ln \frac{p_1^+ - q^+}{p_1^+} \} \\
& + \sum_{q^+ > p_1^+} \left\{ \left[\frac{1}{q^+} + \frac{2}{p_1^+ + p_2^+ - q^+} + \frac{1}{q^+ - p_1^+} \right] \left(\ln(\delta p_{12}^2 e^\gamma) + \ln \frac{p_1^+ + p_2^+ - q^+}{p_1^+ + p_2^+} \right) \right. \\
& + \left[\frac{2}{q^+} + \frac{1}{p_1^+ + p_2^+ - q^+} + \frac{1}{p_1^+ - q^+} \right] \ln \frac{q^+}{p_1^+ + p_2^+} \\
& \left. + \left[\frac{2}{q^+ - p_1^+} + \frac{1}{p_1^+ + p_2^+ - q^+} - \frac{1}{q^+} \right] \ln \frac{q^+ - p_1^+}{p_2^+} \right\} \tag{51}
\end{aligned}$$

The first term on the right of (48) must be canceled by a counterterm, since it violates Lorentz invariance. The required counterterm has the form

$$\Gamma_{\text{C.T.}}^{\wedge\wedge\vee} = + \frac{(g\sqrt{N_c})^3}{12\pi^2} (k_0^\wedge + k_1^\wedge + k_2^\wedge) \tag{52}$$

which is completely symmetric in the three legs. We now show how it can be described in the worldsheet formalism. The lightcone worldsheet for the cubic vertex is a rectangle with a cut represented by a solid line as in Fig. 8. Each dual momentum \mathbf{k}_i is the boundary value of $\mathbf{q}(\sigma, \tau)$ on one of the three boundaries: the left side of the rectangle, the cut in the middle, and the right side of the rectangle. For definiteness we assign these boundaries the label $i = 0, 1, 2$, so \mathbf{k}_i is the boundary value at boundary i . The cubic vertex is characterized by the point on the worldsheet where the cut terminates. The value of \mathbf{q} on the cut is \mathbf{k}_1 and by continuity it has this value at the termination point. Thus we can write $q^\wedge(A) = k_1^\wedge$. That is k_1^\wedge is locally associated with the vertex but k_0^\wedge and k_2^\wedge are not. However an insertion of $\partial q^\wedge / \partial \sigma$ into the worldsheet path integral of a single gluon produces the factor [5]

$$\left\langle \frac{\partial q^\wedge}{\partial \sigma} \right\rangle = \frac{\Delta q^\wedge}{p^+} \tag{53}$$

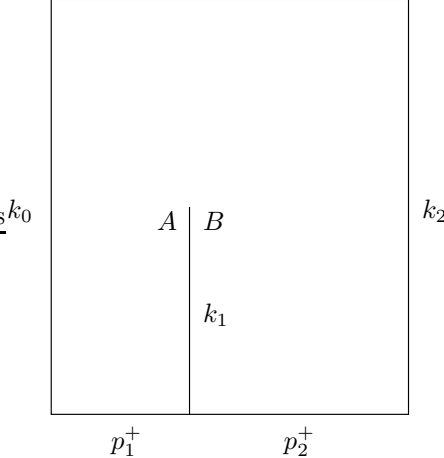


Figure 8: The lightcone worldsheet for the cubic vertex

where Δq^\wedge is the difference of the boundary values at the two boundaries of the gluon worldsheet. Thus we have

$$\left\langle \frac{\partial q^\wedge}{\partial \sigma} \right\rangle_{01} = \frac{k_1^\wedge - k_0^\wedge}{p_1^+} \quad (54)$$

$$\left\langle \frac{\partial q^\wedge}{\partial \sigma} \right\rangle_{12} = \frac{k_2^\wedge - k_1^\wedge}{p_2^+} \quad (55)$$

where the ij subscript means that the insertion is somewhere between boundaries i and j , p_i^+ the $+$ momentum carried by the left gluon is the width of the left gluon strip, and p_2^+ is the width of the right gluon strip. Since it doesn't matter exactly where the insertion occurs we are free to make it arbitrarily close to the end of the internal boundary, say the points A, B in the figure. Thus we can write the counterterm

$$\Gamma_{\text{C.T.}}^{\wedge\wedge\vee} = +\frac{(g\sqrt{N_c})^3}{12\pi^2} \left[3q^\wedge(A) + p_2^+ \left\langle \frac{\partial q^\wedge}{\partial \sigma}(B) \right\rangle - p_1^+ \left\langle \frac{\partial q^\wedge}{\partial \sigma}(A) \right\rangle \right] \quad (56)$$

This is still not quite a local worldsheet modification because of the factors p_i^+ . But as shown in [5] these factors can be locally reproduced by inserting worldsheet ghost fields near the interaction point. Thus the required counterterm has a local worldsheet representation. Including the counterterm we then have for the complete vertex function

$$\Gamma_{1 \text{ loop}} + \Gamma_{\text{C.T.}} = -\frac{g^2 N_c}{8\pi^2} \Gamma_{\text{tree}} \left(\frac{70}{9} - \frac{11}{3} \ln(\delta p_o^2 e^\gamma) + S \right) + \alpha \frac{(g\sqrt{N_c})^3}{12\pi^2} \frac{K}{p_o^+} \quad (57)$$

In addition to these corrections to the tree level cubic vertex, the triangle diagram with three like-helicities (see Fig. 9) is non-zero, and it is given, for the case of two on-shell legs, by

$$\Gamma_{\triangle}^{\wedge\wedge\wedge} = -\frac{(g\sqrt{N_c})^3}{6\pi^2} \frac{K^{\wedge 3}}{p_1^+ p_2^+ p_3^+ p_o^2} \quad (58)$$

$$\Gamma_{\triangle}^{\vee\vee\vee} = -\frac{(g\sqrt{N_c})^3}{6\pi^2} \frac{K^{\vee 3}}{p_1^+ p_2^+ p_3^+ p_o^2} \quad (59)$$

where p_o is the momentum of the off-shell gluon.

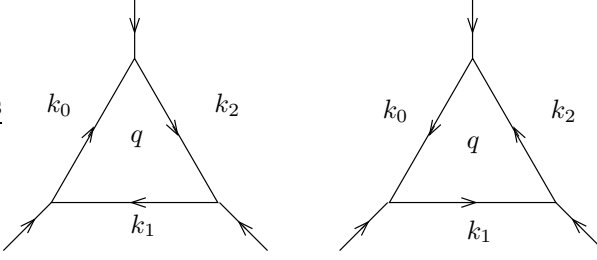


Figure 9: The triangle diagrams contributing to $\Gamma^{\wedge\wedge\wedge}$.

7 Reduction of Box Diagrams

We have seen that the on-shell limit of a tree amplitude is dramatically simpler than the off-shell expression. We can identify tree amplitudes as sub-diagrams of one loop diagrams, but some of the legs of these sub-diagrams will be off-shell, so it would seem that the simplifying features of the on-shell limit can't be exploited. However, if one leaves the denominators of the trees in their original covariant form, then the numerators can always be written as the simplified on-shell expression plus terms each of which contain at least one factor of the virtuality p^2 of one of the off-shell legs. In a box diagram such terms will cancel a propagator reducing the required loop integrand to one with the structure of a triangle diagram. Since triangle integrals are considerably easier to analyze than box integrals, the resulting simplification is very useful. In this section, we use this technique to reduce the complications of the box diagrams for the helicity configurations $\wedge\wedge\wedge\wedge$ and $\wedge\wedge\wedge\vee$, which are the focus of this article. For these spin configurations we can always find a four point sub-diagram of the box diagram that involves helicities $\wedge\wedge\wedge\vee$ or $\wedge\vee\vee\vee$, as indicated in Figure 10. Thus these box diagrams can be completely reduced to triangle-type integrals.

7.1 $\wedge\wedge\wedge\wedge$

Referring to the first line of Fig. 10, and remembering that there is one other box contribution with the arrows circulating clockwise with the same value, we read off the box contribution to the four like helicity process:

$$\Gamma_{\text{Box}}^{\wedge\wedge\wedge\wedge} = 2(2g)^4 N_c^2 \int \frac{d^4 q}{16\pi^4} \frac{K_{12}^\wedge K_{35}^\wedge K_{64}^\wedge}{p_1^+ p_2^+ p_3^+ p_4^+ p_{12}^2} \left[\frac{K_{25}^\wedge}{q_1^2 q_2^2 q_3^2} + \frac{K_{61}^\wedge}{q_0^2 q_2^2 q_3^2} - \frac{K_{61}^\wedge + K_{25}^\wedge - K_{12}^\wedge}{q_0^2 q_2^2 q_3^2} \right] \quad (60)$$

where the off-shell momenta are defined as $p_5 = q - k_2$, $p_6 = k_0 - q$ and $q_i^2 = (q - k_i)^2$.

7.2 $\wedge\wedge\wedge\vee$

Here we gather the triangle-like contributions arising from the five box diagrams contributing to the process with three like helicities (see the second and third lines of Fig. 10). In the loop integrand, there are four distinct triangle denominator structures descended from the box denominators $(q_0^2 q_1^2 q_2^2 q_3^2)^{-1}$. We list the coefficient of each structure. The coefficient of $g^4 N_c^2 (\pi^4 q_0^2 q_1^2 q_3^2)^{-1}$ is

$$\begin{aligned} & \frac{K_{12}^\wedge K_{61}^\wedge K_{64}^\vee K_{35}^\wedge}{p_1^+ p_2^+ p_3^+ p_4^+ p_{12}^2} \left[\frac{q^{+2}}{(q^+ + p_4^+)^2} + \frac{(q^+ + p_4^+)^2}{q^{+2}} \right] + \frac{K_{12}^\wedge K_{61}^\wedge K_{64}^\wedge K_{35}^\vee}{p_1^+ p_2^+ p_3^+ p_4^+ p_{12}^2} \frac{p_3^{+2} p_4^{+2}}{(q^+ - p_{12}^+)^2 (q^+ + p_4^+)^2} \\ & + \frac{K_{34}^\wedge K_{61}^\wedge K_{64}^\wedge K_{25}^\vee}{p_1^+ p_2^+ p_3^+ p_4^+ p_{12}^2} \frac{p_2^{+2} p_4^{+2}}{(q^+ - p_1^+)^2 (q^+ - p_{12}^+)^2} + \frac{K_{34}^\wedge K_{61}^\wedge K_{64}^\wedge K_{25}^\wedge}{p_1^+ p_2^+ p_3^+ p_4^+ p_{12}^2} \frac{p_1^{+2} p_4^{+2}}{(q^+ - p_1^+)^2 q^{+2}}. \end{aligned} \quad (61)$$

The coefficient of $g^4 N_c^2 (\pi^4 q_1^2 q_2^2 q_3^2)^{-1}$ is

$$\frac{K_{12}^\wedge K_{25}^\wedge K_{64}^\vee K_{35}^\wedge}{p_1^+ p_2^+ p_3^+ p_4^+ p_{12}^2} \left[\frac{q^{+2}}{(q^+ + p_4^+)^2} + \frac{(q^+ + p_4^+)^2}{q^{+2}} \right] + \frac{K_{12}^\wedge K_{25}^\wedge K_{64}^\wedge K_{35}^\vee}{p_1^+ p_2^+ p_3^+ p_4^+ p_{12}^2} \frac{p_3^{+2} p_4^{+2}}{(q^+ - p_{12}^+)^2 (q^+ + p_4^+)^2}$$

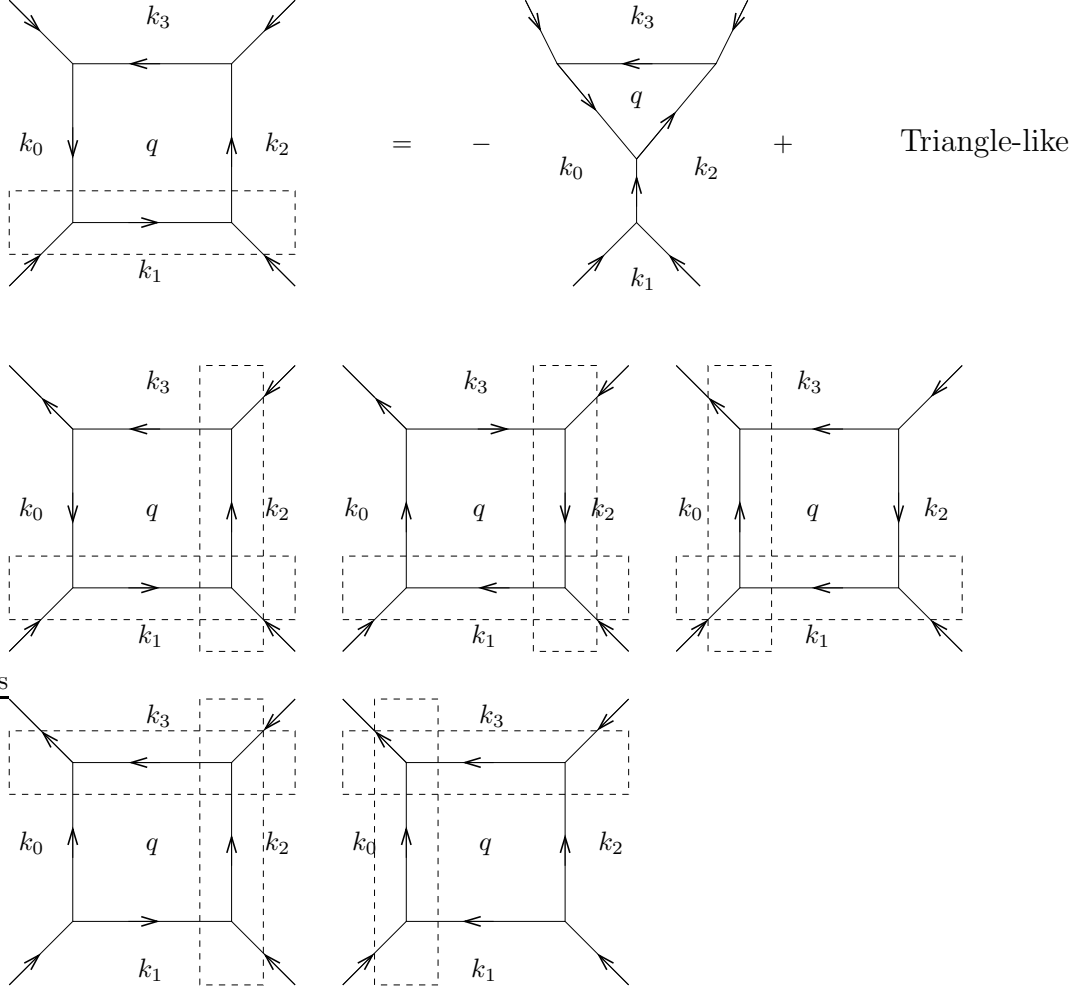


Figure 10: The boxes for the finite one-loop amplitudes can be reduced to triangles and triangle-like integrals by replacing any of the sub-diagrams enclosed in a dashed box. A typical replacement is shown in the first line.

$$+ \frac{K_{34}^\wedge K_{35}^\wedge K_{61}^\wedge K_{25}^\vee}{p_1^+ p_2^+ p_3^+ p_4^+ p_{12}^2} \frac{p_2^{+2} p_4^{+2}}{(q^+ - p_1^+)^2 (q^+ - p_{12}^+)^2} + \frac{K_{34}^\wedge K_{61}^\vee K_{35}^\wedge K_{25}^\wedge}{p_1^+ p_2^+ p_3^+ p_4^+ p_{12}^2} \frac{p_1^{+2} p_4^{+2}}{(q^+ - p_1^+)^2 q^{+2}}. \quad (62)$$

The coefficient of $g^4 N_c^2 (\pi^4 q_0^2 q_1^2 q_2^2)^{-1}$ is

$$- \frac{K_{34}^\wedge K_{61}^\wedge K_{65}^\wedge K_{25}^\vee}{p_1^+ p_2^+ p_3^+ p_4^+ p_{12}^2} \frac{p_2^{+2} p_4^{+2}}{(q^+ - p_1^+)^2 (q^+ - p_{12}^+)^2} - \frac{K_{34}^\wedge K_{61}^\vee K_{65}^\wedge K_{25}^\wedge}{p_1^+ p_2^+ p_3^+ p_4^+ p_{12}^2} \frac{p_1^{+2} p_4^{+2}}{(q^+ - p_1^+)^2 q^{+2}}. \quad (63)$$

The coefficient of $g^4 N_c^2 (\pi^4 q_0^2 q_2^2 q_3^2)^{-1}$ is

$$- \frac{K_{12}^\wedge K_{56}^\wedge K_{64}^\vee K_{35}^\wedge}{p_1^+ p_2^+ p_3^+ p_4^+ p_{12}^2} \left[\frac{q^{+2}}{(q^+ + p_4^+)^2} + \frac{(q^+ + p_4^+)^2}{q^{+2}} \right] - \frac{K_{12}^\wedge K_{56}^\wedge K_{64}^\wedge K_{35}^\vee}{p_1^+ p_2^+ p_3^+ p_4^+ p_{12}^2} \frac{p_3^{+2} p_4^{+2}}{(q^+ - p_{12}^+)^2 (q^+ + p_4^+)^2}. \quad (64)$$

8 $\wedge \wedge \wedge \wedge$ at One Loop

8.1 Direct Calculation of the Box and Triangle contributions

Because the tree contribution to this process is zero, the one loop contribution must be completely finite. The triangle-like integral descended from the box diagrams is spelled out in Eq. (60). The integral over q is finite and can be explicitly evaluated. The last term in Eq. (60) can be identified (note that $K_{61}^\wedge + K_{25}^\wedge - K_{12}^\wedge = K_{56}^\wedge$) as the negative of the pure triangle diagram attached to legs 3 and 4. So, when added to the triangle diagrams attached to legs 3 and 4, this term is canceled out so the box and this triangle diagram together become

$$g^4 N_c^2 \int \frac{d^4 q}{\pi^4} \frac{2K_{12}^\wedge K_{64}^\wedge K_{35}^\wedge}{p_1^+ p_2^+ p_3^+ p_4^+ p_{12}^2} \left[\frac{K_{61}^\wedge}{q_0^2 q_1^2 q_3^2} + \frac{K_{25}^\wedge}{q_1^2 q_2^2 q_3^2} \right], \quad (65)$$

which, after integration over q , gives.

$$\frac{g^4 N_c^2}{3\pi^2} \frac{K_{12}^\wedge}{p_1^+ p_2^+ p_3^+ p_4^+ p_{12}^2} [K_{41}^\wedge K_{23}^\wedge (K_{41}^\wedge + K_{23}^\wedge) + K_{34}^\wedge (K_{41}^\wedge)^2 + K_{23}^\wedge)^2]. \quad (66)$$

The remaining triangles are also finite and can easily be calculated. The triangle attached to legs 1 and 2 is

$$\frac{g^4 N_c^2}{3\pi^2} \frac{K_{34}^\wedge K_{12}^\wedge}{p_1^+ p_2^+ p_3^+ p_4^+ p_{12}^4}. \quad (67)$$

The triangle attached to legs 1 and 4 is

$$\frac{g^4 N_c^2}{3\pi^2} \frac{K_{23}^\wedge K_{41}^\wedge}{p_1^+ p_2^+ p_3^+ p_4^+ p_{14}^4}. \quad (68)$$

And the triangle attached to legs 2 and 3 is

$$\frac{g^4 N_c^2}{3\pi^2} \frac{K_{41}^\wedge K_{23}^\wedge}{p_1^+ p_2^+ p_3^+ p_4^+ p_{14}^4}. \quad (69)$$

As explained in the next subsection, the physical one loop scattering amplitude contains no self energy insertions, and so is obtained by adding all these contributions. So, the *physical* one loop scattering amplitude is

$$\begin{aligned} \Gamma^{\wedge \wedge \wedge \wedge} &= \frac{g^4 N_c^2}{3\pi^2} \frac{1}{p_1^+ p_2^+ p_3^+ p_4^+} \left[\frac{K_{12}^\wedge K_{41}^\wedge K_{23}^\wedge (K_{41}^\wedge + K_{23}^\wedge) + K_{12}^\wedge K_{34}^\wedge (K_{41}^\wedge)^2 + K_{23}^\wedge)^2}{p_{12}^2 p_{14}^2} \right. \\ &\quad \left. + \frac{K_{34}^\wedge K_{12}^\wedge}{p_{12}^4} + \frac{K_{23}^\wedge K_{41}^\wedge}{p_{14}^4} + \frac{K_{41}^\wedge K_{23}^\wedge}{p_{14}^4} \right] \\ &= \frac{g^4 N_c^2}{3\pi^2} \frac{1}{p_1^+ p_2^+ p_3^+ p_4^+ p_{12}^2 p_{14}^2} [K_{12}^\wedge K_{41}^\wedge K_{23}^\wedge (K_{41}^\wedge + K_{23}^\wedge) + K_{12}^\wedge K_{34}^\wedge (K_{41}^\wedge)^2 + K_{23}^\wedge)^2 \\ &\quad - K_{12}^\wedge K_{23}^\wedge K_{41}^\wedge - K_{41}^\wedge K_{12}^\wedge K_{34}^\wedge - K_{23}^\wedge K_{12}^\wedge K_{34}^\wedge] \\ &= \frac{g^4 N_c^2}{3\pi^2} \frac{K_{12}^\wedge K_{41}^\wedge K_{23}^\wedge}{p_1^+ p_2^+ p_3^+ p_4^+ p_{12}^2 p_{14}^2} (K_{41}^\wedge + K_{23}^\wedge - K_{12}^\wedge) \\ &= \frac{g^4}{3\pi^2} \frac{K_{12}^\wedge K_{23}^\wedge K_{34}^\wedge K_{41}^\wedge}{p_1^+ p_2^+ p_3^+ p_4^+ p_{12}^2 p_{14}^2} \\ &= - \frac{g_s^4 N_c^2}{48\pi^2} \frac{K_{21}^\wedge K_{43}^\wedge}{K_{21}^\vee K_{43}^\vee} \end{aligned} \quad (70)$$

where $g_s = g\sqrt{2}$ is the conventional QCD coupling constant. Removing a factor of N_c , we find that this result agrees exactly with the known one [16, 17].

8.2 Discussion and a Remarkable Identity

In the previous subsection we identified the physical scattering amplitude with the box and triangle diagrams only. However, our δ regulator leads to a non-zero result for the one loop helicity flipping self energy function $\Pi^{\wedge\wedge}$:

$$\Pi^{\wedge\wedge}(k, k') = \frac{g^2 N_c}{12\pi^2} (k^{\wedge 2} + k^{\wedge} k'^{\wedge} + k'^{\wedge 2}) \quad (71)$$

Here k, k' are the dual momenta assigned to the two external regions separated by the external lines. (With our definitions the conventional $\alpha_s = g^2/2\pi$, or in other words $g = g_s/\sqrt{2}$.) This result for $\Pi^{\wedge\wedge}$ is anomalous in several respects. For one thing it violates the translational symmetry $k, k' \rightarrow k + a, k' + a$. This formal symmetry of the unregulated theory is violated by our δ regulator. It does not disappear as $\delta \rightarrow 0$ because the self energy integral is quadratically divergent by power-counting, so terms of order $O(\delta)$ get multiplied by a factor $1/\delta$ and so survive the limit. These regulator artifacts are not present in the triangle and box diagrams for this process. In addition, the fact that $\Pi^{\wedge\wedge} \neq 0$ on shell would imply a non-zero transition amplitude for a gluon's helicity to flip, which is inconsistent with Lorentz covariance. Fortunately, the result is a finite quadratic polynomial in k, k' , which can be canceled by a local counterterm. To achieve Lorentz invariance this counterterm must be tuned so that $\Pi_{\text{TOT}}^{\wedge\wedge} = 0$, and this justifies the identification of the physical scattering amplitude we made in the previous subsection.

If we don't include this counterterm, however, there is a remarkable property of the one loop integrand for the complete Green function corresponding to this all like-helicity amplitude in the on-shell limit: It is identically zero [15]! To be precise, this means that the sum of the integrands of the box, four triangles, two self-energy bubbles on internal lines and eight self energy bubbles on external lines (see Figs. 11,12), *with a particular routing of momenta through the individual diagrams*, is identically zero if all external legs are put on-shell. It is crucial here to include the diagrams with self-energy insertions on external legs, which have a

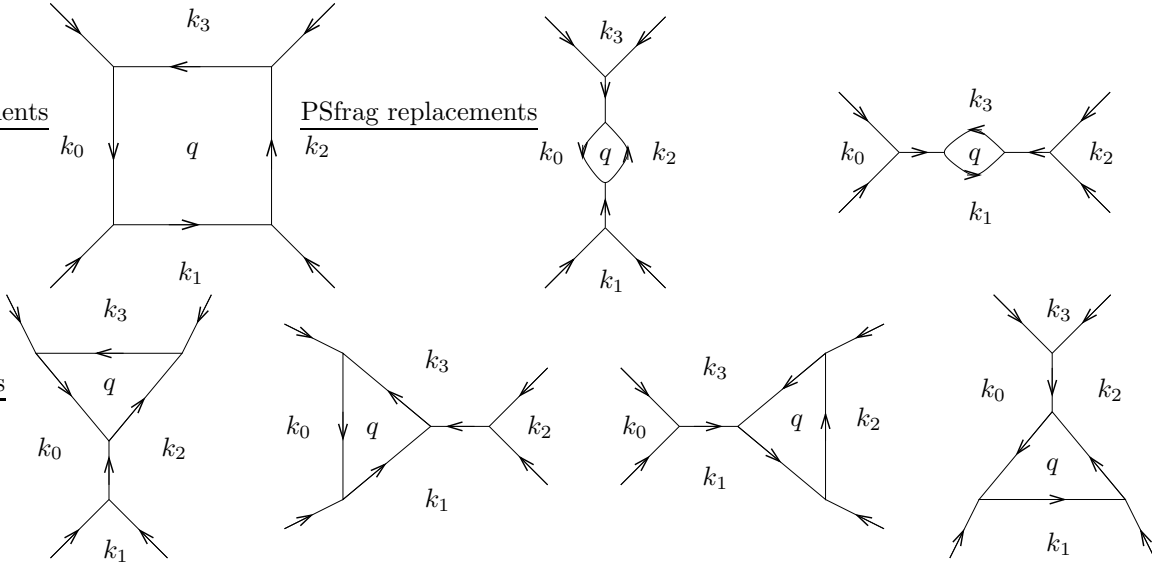


Figure 11: The diagrams contributing to the four point like helicity Green function without bubbles on external legs.

finite on-shell limit because the pole due to the internal line attached to the bubble is canceled by a zero in the on-shell tree amplitude with three like helicities. Because of this remarkable identity, we can interpret the all like helicity scattering amplitude as a pure anomaly arising from the need for counterterms that restore

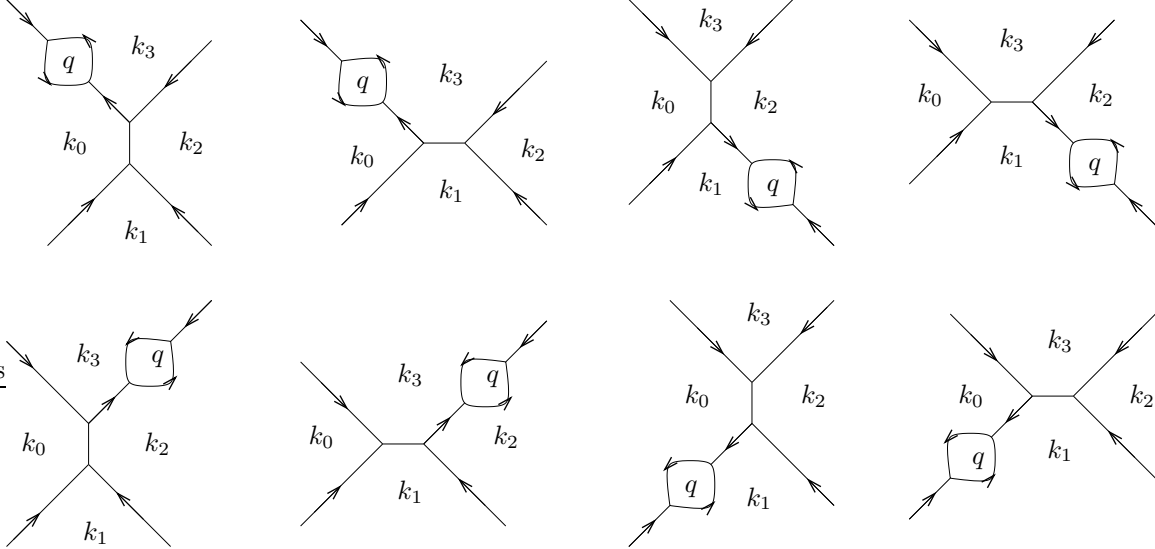


Figure 12: The diagrams contributing to the four point like helicity Green function with bubbles on external legs.

Lorentz invariance. Without the counterterms, the amplitude would vanish, but Lorentz invariance would be violated for other physical processes.⁶

The routing of loop momenta in the individual diagrams that ensures the vanishing of the integrand is indeed the routing dictated by the worldsheet representation [2]. Namely, each diagram divides the plane into the same number of regions, and the dual momentum for each region is assigned identically for each diagram. Then the regulator factor $e^{-\delta q^2}$ is the same for each diagram and doesn't disturb the complete cancellation of the integrand.

To confirm that the sum of the integrands vanishes with the indicated routing of momenta, we note that this sum is a meromorphic function of q^- that vanishes at infinity. It has poles where the denominators vanish with residues that are just on-shell 6 point trees with the pair of legs that correspond to the internal line with the pole under consideration carrying equal and opposite momenta. Since the set of diagrams included does not include tadpole insertions, the six point diagram where these two legs share a common cubic vertex is absent. But these diagrams are zero because of this momentum constraint⁷. Since five legs of the six point trees giving the one loop residues have the same helicity, they all vanish on shell, so all the poles of the meromorphic function have zero residue. This implies that the function is identically zero, and we have seen that residues of the tadpole integrands vanish by themselves so they can be deleted.

⁶In covariant gauge calculations using dimensional regularization, this fact is understood in the following way: The loop integrand vanishes only in four space-time dimensions and only like a single power of $D-4$. UV divergences in the loop integrals become simple poles at $D=4$. These poles are canceled by the zero of the integrand at $D=4$, rendering the amplitude finite but non-zero.

⁷To see this first evaluate the off-shell ($p_5^2 \neq 0$) five-point function, which is easily found to be

$$A_{\wedge\wedge\wedge\wedge\vee}^{\text{tree}} = -\frac{p_2^+ p_3^+ p_5^+}{8K_{43}^\vee K_{32}^\vee K_{21}^\vee} p_5^2 \quad (72)$$

which of course vanishes on shell. We then get these diagrams by multiplying by $-K_{76}^\wedge p_7^+ / (p_5^+ p_6^+ p_5^2)$, which is the 567 vertex times the propagator for leg 5. Thus residue of the pole in the tadpole integrand is the $p_7 \rightarrow -p_6$ limit of

$$R_{\text{tadpole}} = \frac{p_2^+ p_3^+ p_7^+}{8p_6^+ K_{43}^\vee K_{32}^\vee K_{21}^\vee} K_{76}^\wedge \rightarrow 0 \quad (73)$$

We close this section by demonstrating these results by direct calculation. The four poles in q^- are given by $(q - k_i)^2 = 0$ for each $i = 0, 1, 2, 3$. If the residue of any one of these poles is zero, it follows from symmetry that the other three residues are also zero. So we need only consider the first pole with $i = 0$. The diagrams that give this pole are the box, three of the triangles, one of the internal self energies and four of the external self energies: namely all the diagrams with an internal line bordering the region labeled k_0 . The cyclic ordering of the tree is then 123456 where 1234 label the external legs of the loop diagram and $p_5 = -p_6 = q - k_0$.

Using our expression for the off-shell four point function it is convenient to group the contributing diagrams into:

1. The four external self energy diagrams which sum and simplify to

$$\frac{p_5^{+2}}{8} \left[-\frac{p_3^+}{p_5^+} \frac{K_{51}^\wedge}{K_{51}^\vee K_{43}^\vee K_{32}^\vee} + \frac{p_2^+}{p_5^+} \frac{K_{54}^\wedge}{K_{54}^\vee K_{21}^\vee K_{32}^\vee} \right] \quad (74)$$

where we have made use of $p_6 = -p_5$. Notice that the explicit factor of p^2 in the off-shell four point function cancels the propagator factor $1/p^2$ so this limit is finite. Here $p = p_i + p_5 + p_6$ if the bubble is on the i th leg.

2. The four diagrams that also have the propagator $(q - k_2)^{-2}$ (the box, two of the triangles and the internal self energy). These diagrams all together give the product of two off-shell four point functions times this propagator:

$$\frac{p_5^{+2}}{8} \left[\frac{p_1^+ p_4^+ (p_3 + p_4 + p_5)^2}{2 K_{51}^\vee K_{21}^\vee K_{43}^\vee K_{45}^\vee} \right] \quad (75)$$

3. The third triangle diagram:

$$\frac{p_5^{+2}}{8} \left[\frac{K_{21}^\wedge + K_{52}^\wedge + K_{31}^\wedge + K_{53}^\wedge}{K_{51}^\vee K_{32}^\vee K_{54}^\vee} \right] \quad (76)$$

We have omitted coupling constant factors $(2g\sqrt{N_c})^4$ in the above expressions. The claim is that the sum of all these contributions is zero. Putting them all over a common denominator, we see immediately that the terms independent of p_5 sum to zero:

$$(K_{21}^\wedge + K_{31}^\wedge) K_{21}^\vee K_{43}^\vee - \frac{p_1^+ p_4^+ (p_3 + p_4)^2 K_{32}^\vee}{2} = K_{43}^\vee p_1^+ \left(-\frac{1}{p_1^+} K_{41}^\wedge K_{21}^\vee + \frac{1}{p_3^+} K_{43}^\wedge K_{32}^\vee \right) = 0 \quad (77)$$

This leaves

$$\begin{aligned} & \frac{p_5^{+2}}{8 K_{51}^\vee K_{21}^\vee K_{43}^\vee K_{32}^\vee K_{54}^\vee} \left[-\frac{p_3^+}{p_5^+} (K_{51}^\wedge K_{21}^\vee K_{54}^\vee) + \frac{p_2^+}{p_5^+} (K_{54}^\wedge K_{51}^\vee K_{43}^\vee) \right. \\ & \left. - p_1^+ p_4^+ p_5 \cdot (p_3 + p_4) K_{32}^\vee + (K_{52}^\wedge + K_{53}^\wedge) K_{21}^\vee K_{43}^\vee \right] \end{aligned} \quad (78)$$

A systematic way to see that these terms also cancel is to use the identities

$$p_4^+ K_{51}^\vee + p_1^+ K_{45}^\vee + p_5^+ K_{14}^\vee = 0 \quad (79)$$

$$p_4^+ K_{53}^\vee + p_3^+ K_{45}^\vee + p_5^+ K_{34}^\vee = 0 \quad (80)$$

to isolate the dependence on p_5^\vee . Then the quantity in square brackets reads

$$\left[\quad \right] = K_{54}^\vee \frac{p_1^+ p_3^+}{p_4^+} \sum_i \frac{K_{5i}^\wedge K_{i2}^\wedge}{p_i^+} + K_{43}^\vee \left[p_2^+ \sum_i \frac{K_{5i}^\wedge K_{i1}^\wedge}{p_i^+} + \frac{K_{53}^\wedge}{p_3^+} (p_3^+ K_{21}^\vee + p_1^+ K_{32}^\vee + p_2^+ K_{13}^\vee) \right] = 0 \quad (81)$$

As already stated, symmetry dictates that the residues of the other three poles in q^- also vanish, which then proves that the integrand vanishes identically at all q . If we regulate the loop integrals by a direct cutoff on q , for example by inserting a factor $e^{-\delta q^2}$, it follows that the sum of all the regulated integrals vanishes also.

Incorporating this counterterm, the revised on shell MHV Green function, namely value of the box and four triangle contributions combined, can be identified with the physical scattering amplitude. In view of the fact that the unsubtracted diagrams sum to zero, the physical scattering amplitude is just the negative of the self energy contributions to the on-shell Green function. Thus we can calculate the scattering amplitude by a purely algebraic combination of the numerous self-energy insertions. For the reader's entertainment We list the evaluation of these simple diagrams.

1. Bubbles on internal lines:

$$\frac{(p_1^+ + p_2^+)^2 K_{14}^\wedge K_{32}^\wedge (k_0^\wedge k_2^\wedge + k_0^\wedge k_3^\wedge + k_2^\wedge k_3^\wedge) + (p_1^+ + p_4^+)^2 K_{21}^\wedge K_{43}^\wedge (k_1^\wedge k_3^\wedge + k_1^\wedge k_2^\wedge + k_2^\wedge k_3^\wedge)}{p_1^+ p_2^+ p_3^+ p_4^+ st} \quad (82)$$

2. Bubble on leg 4:

$$\frac{-p_4^{+2} K_{32}^\wedge K_{21}^\wedge (k_0^\wedge k_3^\wedge + k_2^\wedge k_3^\wedge + k_3^\wedge k_2^\wedge)}{p_1^+ p_2^+ p_3^+ p_4^+ st} = \frac{[-p_4^+ p_3^+ K_{14}^\wedge K_{21}^\wedge + p_4^+ (p_3^+ + p_2^+) K_{43}^\wedge K_{21}^\wedge] (k_0^\wedge k_3^\wedge + k_2^\wedge k_3^\wedge + k_3^\wedge k_2^\wedge)}{p_1^+ p_2^+ p_3^+ p_4^+ st} \quad (83)$$

3. Bubble on leg 3:

$$\frac{-p_3^{+2} K_{14}^\wedge K_{21}^\wedge (k_2^\wedge k_3^\wedge + k_2^\wedge k_1^\wedge + k_3^\wedge k_1^\wedge)}{p_1^+ p_2^+ p_3^+ p_4^+ st} \quad (84)$$

4. Bubble on leg 2:

$$\frac{-p_2^{+2} K_{14}^\wedge K_{43}^\wedge (k_1^\wedge k_2^\wedge + k_1^\wedge k_3^\wedge + k_2^\wedge k_3^\wedge)}{p_1^+ p_2^+ p_3^+ p_4^+ st} = \frac{[-p_2^+ p_3^+ K_{14}^\wedge K_{21}^\wedge - p_2^+ (p_1^+ + p_2^+) K_{14}^\wedge K_{32}^\wedge] (k_1^\wedge k_2^\wedge + k_1^\wedge k_3^\wedge + k_2^\wedge k_3^\wedge)}{p_1^+ p_2^+ p_3^+ p_4^+ st} \quad (85)$$

5. Bubble on leg 1:

$$\begin{aligned} & \frac{-p_1^{+2} K_{43}^\wedge K_{32}^\wedge (k_0^\wedge k_1^\wedge + k_0^\wedge k_2^\wedge + k_1^\wedge k_2^\wedge)}{p_1^+ p_2^+ p_3^+ p_4^+ st} = \\ & \frac{[-p_1^+ p_3^+ K_{14}^\wedge K_{21}^\wedge - p_1^+ (p_1^+ + p_4^+) K_{43}^\wedge K_{21}^\wedge - p_1^+ (p_1^+ + p_2^+) K_{14}^\wedge K_{32}^\wedge] (k_0^\wedge k_1^\wedge + k_0^\wedge k_2^\wedge + k_1^\wedge k_2^\wedge)}{p_1^+ p_2^+ p_3^+ p_4^+ st} \end{aligned} \quad (86)$$

We simplify the numerator in sum of all these diagrams in stages

1. Coefficient of $K_{14}^\wedge K_{32}^\wedge$:

$$(p_1^+ + p_2^+) (k_0^\wedge + k_1^\wedge + k_2^\wedge) (p_1^+ (k_2^\wedge - k_1^\wedge) + p_2^+ (k_0^\wedge - k_1^\wedge)) = -K_{21}^\wedge (p_1^+ + p_2^+) (k_0^\wedge + k_1^\wedge + k_2^\wedge) \quad (87)$$

2. Coefficient of $K_{43}^\wedge K_{21}^\wedge$:

$$(p_1^+ + p_4^+) (k_0^\wedge + k_1^\wedge + k_3^\wedge) (p_1^+ (k_3^\wedge - k_0^\wedge) + p_4^+ (k_1^\wedge - k_0^\wedge)) = -K_{14}^\wedge (p_1^+ + p_4^+) (k_0^\wedge + k_1^\wedge + k_3^\wedge) \quad (88)$$

3. Coefficient of $K_{14}^\wedge K_{21}^\wedge$:

$$\begin{aligned} & -p_3^+ [p_4^+ (k_0^\wedge k_3^\wedge + k_2^\wedge k_3^\wedge + k_3^\wedge k_2^\wedge) + p_3^+ (k_2^\wedge k_3^\wedge + k_3^\wedge k_2^\wedge + k_0^\wedge k_3^\wedge) + p_2^+ (k_1^\wedge k_2^\wedge + k_1^\wedge k_3^\wedge + k_2^\wedge k_3^\wedge) + p_1^+ (k_0^\wedge k_1^\wedge + k_0^\wedge k_2^\wedge + k_1^\wedge k_2^\wedge)] \\ & = -p_3^+ [K_{43}^\wedge (k_0^\wedge + k_2^\wedge + k_3^\wedge) + K_{21}^\wedge (k_0^\wedge + k_1^\wedge + k_2^\wedge)] \end{aligned} \quad (89)$$

Putting the numerator all together we have

$$\begin{aligned}
N &= K_{14}^\wedge K_{21}^\wedge [-K_{32}^\wedge(p_1^+ + p_2^+)(k_0^\wedge + k_1^\wedge + k_2^\wedge) - K_{43}^\wedge(p_1^+ + p_4^+)(k_0^\wedge + k_1^\wedge + k_3^\wedge) \\
&\quad - p_3^+(K_{43}^\wedge(k_0^\wedge + k_2^\wedge + k_3^\wedge) + K_{21}^\wedge(k_0^\wedge + k_1^\wedge + k_2^\wedge))] \\
&= K_{14}^\wedge K_{21}^\wedge K_{43}^\wedge [p_2^+(k_3^\wedge - k_2^\wedge) + p_3^+(k_1^\wedge - k_2^\wedge)] = -K_{14}^\wedge K_{21}^\wedge K_{43}^\wedge K_{32}^\wedge
\end{aligned} \tag{90}$$

So, restoring the coupling factors, the physical scattering amplitude is the negative of this

$$\begin{aligned}
\Gamma^{\wedge\wedge\wedge\wedge} &= +N_c(2g)^2 \frac{g^2 N_c}{12\pi^2} \frac{K_{14}^\wedge K_{21}^\wedge K_{43}^\wedge K_{32}^\wedge}{p_1^+ p_2^+ p_3^+ p_4^+ s t} = -N_c(2g)^2 \frac{g^2 N_c}{12\pi^2} \frac{K_{21}^\wedge K_{43}^\wedge}{p_1^+ p_2^+ p_3^+ p_4^+ s^2} \\
&= -\frac{g^4 N_c^2}{12\pi^2} \frac{K_{21}^\wedge K_{43}^\wedge}{K_{21}^\vee K_{43}^\vee} = -\frac{g_s^4 N_c^2}{48\pi^2} \frac{K_{21}^\wedge K_{43}^\wedge}{K_{21}^\vee K_{43}^\vee}
\end{aligned} \tag{91}$$

in agreement with (70).

9 $\wedge \wedge \wedge \vee$ at One Loop

9.1 Cubic Vertex corrections and self energy insertions on internal lines.

The one loop corrections to the cubic vertices have the topology of triangle and swordfish diagrams. They have been evaluated in [14] and quoted in Section 6. With the definitions given in Section 6 we now summarize the cubic vertex corrections to on-shell scattering of glue by glue:

$$\begin{aligned}
\frac{\Gamma_\Delta^{\wedge\wedge\wedge\vee}}{16g^4 N_c^2} &= -\frac{p_4^+}{32\pi^2 p_1^+ p_2^+ p_3^+} \left\{ \frac{K_{34}^\wedge K_{12}^\wedge}{p_{12}^2} \left[\frac{22}{3} \ln(p_{12}^2 e^\gamma \delta) - \frac{140}{9} - S_3^{q^+}(p_1, p_2) - S_3^{q^+}(-p_4, -p_3) + \frac{p_1^+ p_2^+}{3p_{12}^{+2}} \right] \right. \\
&\quad + \frac{K_{23}^\wedge K_{41}^\wedge}{p_{14}^2} \left[\frac{22}{3} \ln(p_{14}^2 e^\gamma \delta) - \frac{140}{9} - S_2^{q^+}(-p_4, -p_{23}) - S_1^{q^+ + p_4^+}(p_{14}, p_2) + \frac{p_2^+ p_3^+}{3p_{14}^{+2}} \right] \left. \right\} \\
&\quad + \frac{p_3^+}{48\pi^2 p_1^+ p_2^+ p_4^+ p_{12}^{+2}} \frac{K_{12}^{\wedge 3} K_{34}^\vee}{p_{12}^4} + \frac{p_1^+}{48\pi^2 p_2^+ p_3^+ p_4^+ p_{14}^{+2}} \frac{K_{23}^{\wedge 3} K_{41}^\vee}{p_{14}^4}
\end{aligned} \tag{92}$$

where we stress that the cubic counterterm has been included. Finally we give the self energy insertions on internal lines obtained in Section 5, again including the counterterm that sets to zero the helicity flip self energy as well as the boundary counterterm and the gluon mass counterterm:

$$\begin{aligned}
\frac{\Gamma_{\text{SE}}^{\wedge\wedge\wedge\vee}}{16g^4 N_c^2} &= -\frac{p_4^+}{16\pi^2 p_1^+ p_2^+ p_3^+} \left\{ \frac{K_{34}^\wedge K_{12}^\wedge}{p_{12}^2} \left[\mathcal{A}^{q^+}(p_{12}^2, p_{12}^+) - \frac{11}{6} \ln(p_{12}^2 e^\gamma \delta) + \frac{67}{18} \right] \right. \\
&\quad + \frac{K_{23}^\wedge K_{41}^\wedge}{p_{14}^2} \left[\mathcal{A}^{q^+ + p_4^+}(p_{14}^2, p_{14}^+) - \frac{11}{6} \ln(p_{14}^2 e^\gamma \delta) + \frac{67}{18} \right] \left. \right\}
\end{aligned} \tag{93}$$

$$\mathcal{A}^{q^+}(p^2, p^+) = \sum_{q^+} \left[\frac{1}{q^+} + \frac{1}{p^+ - q^+} \right] \ln \left\{ \frac{q^+}{p^+} \left(1 - \frac{q^+}{p^+} \right) p^2 e^\gamma \delta \right\} \tag{94}$$

where the superscript on \mathcal{A} signifies that longitudinal momentum on the internal line on the left with $p^+ > 0$ and time running up.

9.2 Quartic Triangle Diagrams

The four topologies of “quartic triangle” diagrams are shown in Fig. 9. We sketch their evaluation here with more details found in [14]. The coefficient of $16g^4 N_c^2 (16\pi^4 q_0^2 q_1^2 q_3^2)^{-1}$ in the loop integrand is

$$K_{61}^\wedge K_{64}^\wedge \frac{p_4^+ [p_2^+(q^+ + p_4^+) + p_3^+(p_1^+ - q^+)]}{2p_1^+(p_1^+ - q^+)(q^+ + p_4^+)(p_{12}^+ - q^+)^2} \tag{95}$$

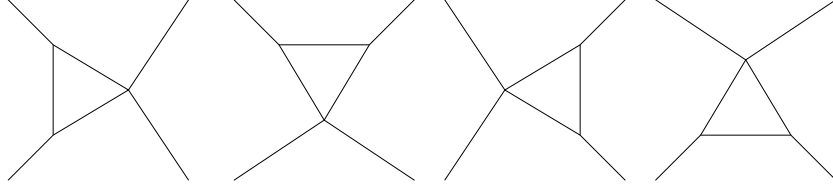


Figure 13: The quartic triangle diagrams shown generically, without arrows indicating spin flow. Particle labels 1234 are applied counter-clockwise starting at the lower left of each diagram.

Integrating over q^- , \mathbf{q} produces, assuming $p_{14}^+ > 0$,

$$\begin{aligned}
\frac{\Gamma_{23}^{\wedge\wedge\wedge\wedge}}{16g^4N_c^2} &= \frac{K_{41}^{\wedge 2}}{32\pi^2 p_1^+ p_{14}^2} \left\{ \sum_{q^+ < -p_4^+} \frac{-q^+}{(p_1^+ - q^+)} \left[\frac{p_2^+ (p_4^+ + q^+) + p_3^+ (p_1^+ - q^+)}{(q^+ + p_4^+) (q^+ - p_{12}^+)^2} \right] \right. \\
&\quad \left. + \sum_{p_1^+ > q^+ > -p_4^+} \frac{p_4^+}{p_{14}^+} \left[\frac{p_2^+ (p_4^+ + q^+) + p_3^+ (p_1^+ - q^+)}{(q^+ + p_4^+) (q^+ - p_{12}^+)^2} \right] \right\} \\
&= \frac{K_{41}^{\wedge 2}}{32\pi^2 p_1^+ p_{14}^2} \left\{ \sum_{q^+ < -p_4^+} \left[-\frac{p_1^+}{p_2^+ (p_1^+ - q^+)} + \frac{p_4^+}{p_3^+ (q^+ + p_4^+)} + \frac{p_2^+ p_4^+ + p_1^+ p_3^+}{p_2^+ p_3^+ (p_{12}^+ - q^+)} + \frac{2p_{12}^+}{(p_{12}^+ - q^+)^2} \right] \right. \\
&\quad \left. + \sum_{p_1^+ > q^+ > -p_4^+} \left[+\frac{p_4^+}{p_3^+ (q^+ + p_4^+)} + \frac{p_4^+}{p_3^+ (p_{12}^+ - q^+)} + \frac{2p_2^+ p_4^+}{p_{14}^+ (p_{12}^+ - q^+)^2} \right] \right\} \\
&\rightarrow \frac{K_{41}^{\wedge 2}}{32\pi^2 p_1^+ p_{14}^2} \left[\frac{p_1^+}{p_2^+} \ln \frac{p_{12}^+ p_{14}^+}{p_1^+ |p_3^+|} + \frac{p_4^+}{p_3^+} \ln \frac{p_{12}^+ p_{14}^+}{p_2^+ |p_4^+|} \right] \tag{96}
\end{aligned}$$

The coefficient of $16g^4N_c^2(16\pi^4 q_0^2 q_2^2 q_3^2)^{-1}$ is

$$K_{35}^{\wedge} K_{64}^{\wedge} \frac{p_4^+ [p_1^+ (q^+ - p_{12}^+) - p_2^+ q^+]}{2p_3^+ (p_{12}^+ - q^+) q^+ (p_1^+ - q^+)^2} \tag{97}$$

and integration gives

$$\begin{aligned}
\frac{\Gamma_{12}^{\wedge\wedge\wedge\wedge}}{16g^4N_c^2} &= \frac{K_{34}^{\wedge 2}}{32\pi^2 p_3^+ p_{12}^+ p_{14}^2} \left\{ \sum_{q^+ < -p_4^+} \frac{p_3^+}{(p_{12}^+ - q^+)} \left[\frac{p_1^+ (p_{12}^+ - q^+) + p_2^+ q^+}{(q^+ - p_1^+)^2} \right] \right. \\
&\quad \left. + \sum_{q^+ > -p_4^+} \frac{p_4^+}{q^+} \left[\frac{p_1^+ (p_1^+ + p_2^+ - q^+) + p_2^+ q^+}{(q^+ - p_1^+)^2} \right] \right\} \tag{98}
\end{aligned}$$

$$\begin{aligned}
&= \frac{K_{34}^{\wedge 2}}{32\pi^2 p_3^+ p_{12}^+ p_{14}^2} \left\{ \sum_{q^+ < -p_4^+} \left[\frac{p_3^+ p_{12}^+}{p_2^+ (p_{12}^+ - q^+)} + \frac{2p_1^+ p_3^+}{(q^+ - p_1^+)^2} + \frac{p_3^+ p_{12}^+}{p_2^+ (q^+ - p_1^+)} \right] \right. \\
&\quad \left. + \sum_{q^+ > -p_4^+} \left[\frac{p_{12}^+ p_4^+}{p_1^+ q^+} + \frac{2p_2^+ p_4^+}{(q^+ - p_1^+)^2} + \frac{p_{12}^+ p_4^+}{p_1^+ (p_1^+ - q^+)} \right] \right\} \tag{99}
\end{aligned}$$

$$\rightarrow \frac{K_{34}^{\wedge 2}}{32\pi^2 p_3^+ p_{12}^2} \left\{ \frac{1}{p_{12}^+} \sum_{q^+ > -p_4^+} \frac{2p_2^+ p_4^+}{(q^+ - p_1^+)^2} - \frac{2p_3^+ p_4^+}{p_{12}^+ p_{14}^+} + \frac{p_1^+ p_3^+ + p_2^+ p_4^+}{p_1^+ p_2^+} \ln \frac{p_{12}^+ p_{14}^+}{p_1^+ p_2^+} \right\} \tag{100}$$

The coefficient of $16g^4N_c^2(16\pi^4 q_1^2 q_2^2 q_3^2)^{-1}$ is

$$K_{25}^{\wedge} K_{35}^{\wedge} \left\{ \frac{(p_1^+ - q^+) [p_4^+ (q^+ - p_1^+) - p_1^+ (q^+ + p_4^+)]}{2p_2^+ p_3^+ (q^+ + p_4^+) (p_1^+ + p_4^+)^2} \right\}$$

$$-\frac{q^+ + p_4^+}{p_1^+ - q^+} \left[\frac{p_1^+(q^+ - p_1^+) - p_4^+(q^+ + p_4^+)}{2p_2^+ p_3^+ (p_1^+ + p_4^+)^2} + \frac{p_1^+ p_4^+ + (p_1^+ - q^+)(q^+ + p_4^+)}{2p_2^+ p_3^+ q^{+2}} \right] \} \quad (101)$$

and integration gives

$$\begin{aligned} \frac{\Gamma_{41}^{\wedge\wedge\wedge\wedge}}{16g^4 N_c^2} &= -\frac{K_{23}^{\wedge 2}}{32\pi^2 p_2^+ p_3^+ p_{12}^2} \left\{ \sum_{-p_4^+ < q^+ < p_1^+} \frac{q^+ + p_4^+}{p_{14}^+} \left[\frac{q^+ + p_4^+}{p_1^+ - q^+} \right. \right. \\ &\quad \left(\frac{(q^+ - p_1^+)p_1^+ - (q^+ + p_4^+)p_4^+}{(p_1^+ + p_4^+)^2} + \frac{(q^+ + p_4^+)(p_1^+ - q^+) + p_1^+ p_4^+}{q^{+2}} \right) - \frac{p_1^+ - q^+}{q^+ + p_4^+} \frac{(q^+ - p_1^+)p_4^+ - (q^+ + p_4^+)p_1^+}{(p_1^+ + p_4^+)^2} \\ &\quad + \sum_{q^+ > p_1^+} \frac{p_{12}^+ - q^+}{p_2^+} \left[\frac{q^+ + p_4^+}{p_1^+ - q^+} \left(\frac{(q^+ - p_1^+)p_1^+ - (q^+ + p_4^+)p_4^+}{(p_1^+ + p_4^+)^2} + \frac{(q^+ + p_4^+)(p_1^+ - q^+) + p_1^+ p_4^+}{q^{+2}} \right) \right. \\ &\quad \left. \left. - \frac{p_1^+ - q^+}{q^+ + p_4^+} \frac{(q^+ - p_1^+)p_4^+ - (q^+ + p_4^+)p_1^+}{(p_1^+ + p_4^+)^2} \right] \right\} \end{aligned} \quad (102)$$

The coefficient of $16g^4 N_c^2 (16\pi^4 q_0^2 q_1^2 q_2^2)^{-1}$ is

$$\begin{aligned} K_{61}^{\wedge} K_{25}^{\wedge} &\left\{ \frac{(p_{12}^+ - q^+)[p_4^+(p_{12}^+ - q^+) + p_3^+ q^+]}{2p_1^+ p_2^+ q^+(p_1^+ + p_2^+)^2} \right. \\ &\quad \left. - \frac{q^+}{p_{12}^+ - q^+} \left[\frac{q^+(p_{12}^+ - q^+) + p_3^+ p_4^+}{2p_1^+ p_2^+ (q^+ + p_4^+)^2} + \frac{q^+ p_4^+ + (p_{12}^+ - q^+) p_3^+}{2p_1^+ p_2^+ (p_1^+ + p_2^+)^2} \right] \right\} \end{aligned} \quad (103)$$

and integration gives

$$\begin{aligned} \frac{\Gamma_{34}^{\wedge\wedge\wedge\wedge}}{16g^4 N_c^2} &= -\frac{K_{12}^{\wedge 2}}{32\pi^2 p_1^+ p_2^+ p_{12}^2 p_{12}^2} \left\{ \sum_{q^+ < p_1^+} \left[\frac{q^{+2}}{p_1^+(p_{12}^+ - q^+)} \left(\frac{q^+ p_4^+ + (p_{12}^+ - q^+) p_3^+}{(p_1^+ + p_2^+)^2} + \frac{q^+ (p_{12}^+ - q^+) + p_3^+ p_4^+}{(q^+ + p_4^+)^2} \right) \right. \right. \\ &\quad \left. \left. - \frac{(p_{12}^+ - q^+) (q^+ p_3^+ + (p_{12}^+ - q^+) p_4^+)}{p_1^+ (p_1^+ + p_2^+)^2} \right] \right. \\ &\quad + \sum_{q^+ > p_1^+} \left[\frac{q^+}{p_2^+} \left(\frac{q^+ p_4^+ + (p_{12}^+ - q^+) p_3^+}{(p_1^+ + p_2^+)^2} + \frac{q^+ (p_{12}^+ - q^+) + p_3^+ p_4^+}{(q^+ + p_4^+)^2} \right) \right. \\ &\quad \left. \left. - \frac{(p_{12}^+ - q^+)^2 (q^+ p_3^+ + (p_{12}^+ - q^+) p_4^+)}{p_2^+ q^+ (p_1^+ + p_2^+)^2} \right] \right\} \end{aligned} \quad (104)$$

9.3 Result and discussion

Since we already know the results of cubic vertex corrections and self-energy insertion on internal lines, let us concentrate here on the triangle-like contributions originating from the box reduction. Due to kinematic constraints on q^+ , different diagrams live in different patches on the worldsheet. For the discussion let us assume without loss of generality that $p_1^+, p_2^+ > 0$ and $p_1^+ + p_4^+ > 0$. The arguments go similarly for the case $p_1^+ + p_4^+ < 0$. Then we divide the whole worldsheet into three patches $0 \leq q^+ \leq -p_4^+$, $-p_4^+ \leq q^+ \leq p_1^+$ and $p_1^+ \leq q^+ \leq p_{12}^+$. Diagrams with propagators $(q_0^2 q_1^2 q_3^2)^{-1}$ can live only in first two regions ($q^+ < p_1^+$) while the diagrams with $(q_1^2 q_2^2 q_3^2)^{-1}$ live in the second and third regions ($q^+ > -p_4^+$). The diagrams with $(q_0^2 q_2^2 q_3^2)^{-1}$ and $(q_0^2 q_1^2 q_2^2)^{-1}$ live in all three regions. For the calculation, we use Schwinger parameters for the internal propagators and UV cutoff δ as discussed in appendix A and use *Mathematica* to carry out the algebra. To see the cancellation of divergences, it is very helpful to convert all the polarization structures into two independent forms by using the K -identities before summing over q^+ . Using the K -identities, we first express all the K_{ij}^{\wedge} and K_{ij}^{\vee} in terms of K_{12}^{\wedge} and K_{34}^{\wedge} . With K_{12}^{\wedge} and K_{34}^{\wedge} , we can form three bilinear structures $K_{12}^{\wedge 2}$, $K_{34}^{\wedge 2}$ and $K_{12}^{\wedge} K_{34}^{\wedge}$. But, these three bilinears are again related to each other by

$$\frac{K_{12}^{\wedge} K_{34}^{\wedge}}{p_{12}^2} = -\frac{K_{32}^{\wedge} K_{41}^{\wedge}}{p_{14}^2}. \quad (105)$$

Using

$$K_{32}^\wedge = \frac{p_3^+ K_{12}^\wedge - p_2^+ K_{34}^\wedge}{p_{12}^+}, \quad (106)$$

$$K_{41}^\wedge = -\frac{p_4^+ K_{12}^\wedge - p_1^+ K_{34}^\wedge}{p_{12}^+} \quad (107)$$

in Eq. (105) we can eliminate $K_{34}^{\wedge 2}$ by

$$K_{34}^{\wedge 2} = -\frac{p_3^+ p_4^+}{p_1^+ p_2^+} K_{12}^{\wedge 2} + \frac{(p_1^+ p_3^+ + p_2^+ p_4^+) p_{12}^2 + p_{12}^{+2} p_{14}^2}{p_1^+ p_2^+ p_{12}^2} K_{12}^\wedge K_{34}^\wedge. \quad (108)$$

So, we have only two independent polarizations $K_{12}^{\wedge 2}$ and $K_{12}^\wedge K_{34}^\wedge$.

After integrating over q^- , \mathbf{q} and the parameter $T = T_1 + T_2 + T_3$, for each triangle-like term we have an expression of the form

$$\begin{aligned} \sum_{q^+} \int dx_1 dx_2 dx_3 \delta(1 - x_1 - x_2 - x_3) \delta(f(q^+, x_i, p_i^+)) \{ & K_{12}^{\wedge 2} (B_1 + B'_1 \ln(\delta e^\gamma H(x_i x_j p^2))) + \\ & + K_{12}^\wedge K_{34}^\wedge (B_2 + B'_2 \ln(\delta e^\gamma H(x_i x_j p^2))) + K_{12}^\wedge k_i^\wedge B_3^i + K_{34}^\wedge k_i^\wedge B_4^i \}, \end{aligned} \quad (109)$$

where $x_i = T_i/T$. k_i are the dual momenta assigned to the external regions of the loop as shown in Fig. 10 and B_i and B'_i are functions of q^+, p_i^+ and x_i . One can next peacefully perform all the integrations except that over q^+ which we discretize to take care of the singularities. Individually, each diagram is divergent in q^+ in the UV cutoff δ , and does not look simple. But amazing simplifications occur when all diagrams are combined. The physical scattering amplitude $\Gamma^{\wedge\wedge\wedge\wedge\wedge}$ should be proportional to two powers of K_{ij}^\wedge . But in each triangle-like diagram, B_3 and B_4 are proportional to only one power of K_{ij}^\wedge and one power of k_i^\wedge and are not of that form. Nevertheless, when all the allowed triangle-like diagrams in each region on the worldsheet are put together, after integration over the x_i 's, the B_3 and B_4 terms combine nicely to have the appropriate bilinear structures in the K_{ij}^\wedge 's.

From the expressions of the triangle-like diagrams (Eqs. (61)-(64)), we can see that the four possible places where we can encounter divergences are $q^+ = 0, q^+ + p_4^+ = 0, q^+ - p_1^+ = 0$ and $p_{12}^+ - q^+ = 0$. The apparent divergences at the end points $q^+ = 0$ and $p_{12}^+ - q^+ = 0$ are tamed by the limits of integration over the Feynmann parameters x_i , and we need only worry about the singularities at the interior points $q^+ + p_4^+ = 0, q^+ - p_1^+ = 0$. In the first patch of the worldsheet, Eq. (61) and Eq. (64) individually are linearly divergent at $q^+ + p_4^+ = 0$. One part of this divergent term in Eq. (61) cancels the divergence of Eq. (64) and the other part is canceled by the similar term in the quartic triangle $\Gamma_{34}^{\wedge\wedge\wedge\wedge\wedge}$. Similarly in all the three regions, when triangle-like diagrams are combined with the quartic triangle diagrams, all the linear divergences at $q^+ - p_1^+ = 0$ and $q^+ + p_4^+ = 0$ cancel out and we can take the continuum limit of the q^+ sums and perform the resulting integration over q^+ . We also take out the logarithm terms with polynomial coefficients and integrate over q^+ . But, the logarithm terms whose coefficients have q^+ in the denominators are singular and we keep sum over discrete q^+ for them. Those terms are canceled when added with $\Gamma_{\Delta}^{\wedge\wedge\wedge\wedge\wedge}$ and $\Gamma_{SE}^{\wedge\wedge\wedge\wedge\wedge}$. All the triangle-like and quartic triangle terms combine nicely to produce

$$\Gamma_{TL}^{\wedge\wedge\wedge\wedge\wedge} = \frac{(2g)^4 N_c^2}{32\pi^2} \left\{ B_0 + \frac{p_4^+}{p_1^+ p_2^+ p_3^+} \frac{K_{12}^\wedge K_{34}^\wedge}{p_{12}^2} \left[\frac{11}{3} \ln(\delta e^\gamma p_{12}^2) - \frac{11}{3} \ln(\delta e^\gamma p_{14}^2) - S^{q^+}(p_i^+) \right] \right\}, \quad (110)$$

where B_0 is given by

$$\begin{aligned} B_0 = & \left[-\frac{p_1^+(p_2^+ - p_3^+) - 3p_3^+(p_2^+ + p_3^+)}{3p_2^+ p_{12}^+ p_{23}^+ p_4^+ p_{14}^2} - \frac{p_3^+(-3p_1^+ p_{12}^+ + p_3^+(-p_1^+ + p_2^+))}{3p_1^+ p_2^+ p_{12}^+ p_{23}^+ p_4^+ p_{12}^2} \right] K_{12}^{\wedge 2} \\ & + \left[\frac{p_1^+(-p_2^+ + p_3^+) + p_3^+ p_{23}^+}{3p_1^+ p_3^+ p_{23}^+ p_{12}^2} - \frac{p_1^+(-p_2^+ + p_3^+) + 3p_3^+ p_{23}^+}{3p_{12}^+ p_3^+ p_{23}^+ p_4^+ p_{14}^2} \right] K_{12}^\wedge K_{34}^\wedge \end{aligned} \quad (111)$$

and $S^{q^+}(p_i^+)$ contains the terms with logarithms. With a bit rearrangement, it can be written as

$$\begin{aligned} S^{q^+}(p_i^+) &= S_3^{q^+}(p_1, p_2) + S_3^{q^+}(-p_4, -p_3) - S_2^{q^+}(-p_4, -p_{23}) \\ &\quad - S_1^{q^++p_4^+}(p_{14}, p_2) + 2\mathcal{A}^{q^+}(p_{12}^2, p_{12}^+) - 2\mathcal{A}^{q^++p_4^+}(p_{14}^2, p_{14}^+). \end{aligned} \quad (112)$$

The physical scattering amplitude is obtained by adding the box and quartic triangles with all the cubic vertex corrections and the self energy insertions on the internal lines. Then we are just left with

$$\begin{aligned} \Gamma^{\wedge\wedge\wedge\vee} &= \Gamma_{TL}^{\wedge\wedge\wedge\vee} + \Gamma_{\Delta}^{\wedge\wedge\wedge\vee} + \Gamma_{SE}^{\wedge\wedge\wedge\vee} \\ &= (2g)^4 N_c^2 \left\{ \frac{B_0}{32\pi^2} - \frac{p_4^+}{32\pi^2 p_1^+ p_2^+ p_3^+} \frac{K_{34}^\wedge K_{12}^\wedge}{p_{12}^2} \left[\frac{p_1^+ p_2^+}{3p_{12}^{+2}} - \frac{p_2^+ p_3^+}{3p_{14}^{+2}} \right] \right. \\ &\quad \left. + \frac{p_3^+}{48\pi^2 p_1^+ p_2^+ p_4^+ p_{12}^{+2}} \frac{K_{12}^{\wedge 3} K_{34}^\vee}{p_{12}^4} + \frac{p_1^+}{48\pi^2 p_2^+ p_3^+ p_4^+ p_{14}^{+2}} \frac{K_{23}^{\wedge 3} K_{41}^\vee}{p_{14}^4} \right\}. \end{aligned} \quad (113)$$

The above expression simplifies to

$$\begin{aligned} \Gamma^{\wedge\wedge\wedge\vee} &= \frac{(2g)^4 N_c^2}{32\pi^2} \left[\frac{p_2^+ p_3^+ p_{14}^4 + p_1^+ (p_2^+ p_{12}^4 + p_3^+ (p_{12}^2 + p_{14}^2)^2) K_{12}^{\wedge 2}}{3p_1^+ p_2^+ p_{12}^+ p_4^+ p_{12}^4 p_{14}^4} \right. \\ &\quad \left. - \frac{(p_2^+ + p_3^+) p_{12}^2 + (p_1^+ + p_2^+ + 2p_3^+) p_{14}^2}{3p_3^+ p_{12}^+ p_4^+ p_{12}^2 p_{14}^4} K_{12}^\wedge K_{34}^\wedge \right] (p_{12}^2 + p_{14}^2) \end{aligned} \quad (114)$$

which again can be rewritten in the compact form

$$\Gamma^{\wedge\wedge\wedge\vee} = -\frac{g_s^4 N_c^2}{96\pi^2} \frac{p_2^+ p_4^+ K_{13}^{\wedge 2}}{K_{43}^\wedge K_{32}^\vee K_{21}^\vee K_{14}^\wedge} (p_{12}^2 + p_{14}^2) \quad (115)$$

agreeing with the known result [16, 17] after removing a factor of N_c .

Acknowledgments: We would like to thank Zvi Bern for sharing his valuable insight into the structure of gauge theory loop integrands. This work was initiated during the KITP program on QCD and String Theory in Fall 2004, and CBT thanks the Kavli Institute and all participants for providing a stimulating environment. We also thank Lisa Everett and Charlie Sommerfield for critical comments on the manuscript. This research was supported in part by the Department of Energy under Grant No. DE-FG02-97ER-41029.

A Evaluation of Loop Momentum Integrals

The loop integrals we encounter in this article can be most easily handled through the introduction of Schwinger parameters T_1, T_2, T_3, T_4 for the internal line propagators $(q-k_0)^{-2}, (q-k_1)^{-2}, (q-k_2)^{-2}, (q-k_3)^{-2}$ respectively. For the helicity nonconserving processes we have shown that box integrals can always be reduced to triangle-like integrals, which means we will only be integrating three of these parameters setting the fourth to zero. However keeping all four T 's allows us to handle in a unified way the four different triangle topologies we require. We only need remember to set the appropriate one to zero when we do each triangle-like integral. Since some of the diagrams are divergent in the ultraviolet, we also retain the worldsheet UV cutoff factors $e^{-\delta q^2}$. The integral over q^- is equivalent to the insertion of a delta function

$$\int dq^- \rightarrow \pi\delta(T_{14}q^+ - T_2 p_1^+ - T_3 p_{12}^+ + T_4 p_4^+) \quad (116)$$

where we use the shorthand $T_{14} = T_1 + T_2 + T_3 + T_4$. The integration over \mathbf{q} is then a Gaussian that is easily done by completing the square and shifting $\mathbf{q} \rightarrow \mathbf{q} + \mathbf{K}$, with

$$\mathbf{K} = \frac{\mathbf{k}_0 T_1 + \mathbf{k}_1 T_2 + \mathbf{k}_2 T_3 + \mathbf{k}_3 T_4}{T_{14} + \delta} \quad (117)$$

One then finds, using the Feynman parameters $x_i \equiv T_i/T_{14}$ that

$$\mathbf{K}_{16} \rightarrow -p_1^+ \mathbf{q} + q^+ \mathbf{p}_1 - x_3 \mathbf{K}_{12} - x_4 \mathbf{K}_{41} + p_1^+ \frac{\delta \mathbf{K}}{T_{14}} \quad (118)$$

$$\mathbf{K}_{52} \rightarrow -p_2^+ \mathbf{q} + q^+ \mathbf{p}_2 - x_4 \mathbf{K}_{23} - x_1 \mathbf{K}_{12} + p_2^+ \frac{\delta \mathbf{K}}{T_{14}} \quad (119)$$

$$\mathbf{K}_{35} \rightarrow p_3^+ \mathbf{q} - q^+ \mathbf{p}_3 + x_2 \mathbf{K}_{23} + x_1 \mathbf{K}_{34} - p_3^+ \frac{\delta \mathbf{K}}{T_{14}} \quad (120)$$

$$\mathbf{K}_{64} \rightarrow p_4^+ \mathbf{q} - q^+ \mathbf{p}_4 + x_3 \mathbf{K}_{34} + x_2 \mathbf{K}_{41} - p_4^+ \frac{\delta \mathbf{K}}{T_{14}} \quad (121)$$

We shall have use for the following combinations of momenta which arise in the loop integrand after shifting q and sending $\delta \rightarrow 0$

$$K_0 = x_2 p_1 + x_3 (p_1 + p_2) - x_4 p_4 \quad (122)$$

$$K_0 - p_1 = x_3 p_2 + x_4 (p_2 + p_3) - x_1 p_1 \quad (123)$$

$$K_0 - p_1 - p_2 = x_4 p_3 + x_1 (p_3 + p_4) - x_2 p_2 \quad (124)$$

$$K_0 + p_4 = x_1 p_4 + x_2 (p_1 + p_4) - x_3 p_3 \quad (125)$$

It is convenient to change variables to $T = T_{14}$ and the x_i after which the T integral can be done. In the evaluation of triangle-like diagrams there are two x_i to integrate. The q^+ integral is discretized and the corresponding sum over q^+ is always done last. In the evaluation of the on-shell triangle diagram, we encounter integrals of the form

$$\int_{x+y \leq 1} dx dy \delta(q^+ - (x+y)p_1^+ - y p_2^+) \mathcal{I} \quad (126)$$

where the integrand is a linear function of x times a linear function of $\ln xy$, $\ln x(1-x-y)$, or $\ln y(1-x-y)$. By p^+ conservation, two of the momenta $p_{1,2,3}^+$ have one sign and the third has the opposite sign. In this section we label momenta so that $p_1^+ > 0$ and $p_3^+ < 0$ have the same sign. If p_2^+ is positive do the above integral in its displayed form. If p_2^+ is negative rewrite the argument of the delta function in terms of $p_2^+ = -|p_2^+|$ and $p_3^+ = -|p_3^+|$, and rename $x \leftrightarrow y$, which brings the integral to the form

$$\int_{x+y \leq 1} dx dy \delta(q^+ - (x+y)|p_3^+| - y|p_2^+|) \mathcal{I} \quad (127)$$

which reduces it to the first form, with $|p_3^+|$ in the role of p_1^+ and $|p_2^+|$ in the role of p_2^+ . Thus, without loss of generality we can stipulate that $p_1^+, p_2^+ > 0$. Then we do the y integral which sets $y = (q^+ - xp_1^+)/p_{12}^+$, and also sets the range of the x integral $0 < x < x_m$ where $x_m = q^+/p_1^+$ for $q^+ < p_1^+$ and $x_m = (p_{12}^+ - q^+)/p_2^+$ for $q^+ > p_1^+$. Then the following x integrals are needed:

$$\int dx \ln(xy) = \left(x_m - \frac{q^+}{p_1^+} \right) \ln \frac{q^+ - x_m p_1^+}{p_{12}^+} + \frac{q^+}{p_1^+} \ln \frac{q^+}{p_{12}^+} + x_m \ln x_m - 2x_m \quad (128)$$

$$= \begin{cases} \frac{q^+}{p_1^+} \left(\ln \frac{q^+}{p_{12}^+} + \ln \frac{q^+}{p_1^+} - 2 \right) & \text{for } q^+ < p_1^+ \\ \frac{p_{12}^+(p_1^+ - q^+)}{p_1^+ p_2^+} \ln \frac{q^+ - p_1^+}{p_2^+} + \frac{q^+}{p_1^+} \ln \frac{q^+}{p_{12}^+} \\ + \frac{p_{12}^+ - q^+}{p_2^+} \left(\ln \frac{p_{12}^+ - q^+}{p_2^+} - 2 \right) & \text{for } q^+ > p_1^+ \end{cases} \quad (129)$$

$$\int dx x \ln(xy) = \frac{1}{2} \left(x_m^2 - \frac{q^{+2}}{p_1^{+2}} \right) \ln \frac{q^+ - x_m p_1^+}{p_{12}^+} + \frac{q^{+2}}{2p_1^{+2}} \ln \frac{q^+}{p_{12}^+} + \frac{x_m^2}{2} \ln x_m - \frac{x_m^2 p_1^+ + q^+ x_m}{2p_1^+}$$

$$= \begin{cases} \frac{q^{+2}}{2p_1^{+2}} \left(\ln \frac{q^{+}}{p_{12}^{+}} + \ln \frac{q^{+}}{p_1^{+}} - 2 \right) & \text{for } q^{+} < p_1^{+} \\ \frac{p_{12}^{+}(p_1^{+} - q^{+})}{2p_1^{+}p_2^{+}} \left[\frac{q^{+}}{p_1^{+}} + \frac{p_{12}^{+} - q^{+}}{p_2^{+}} \right] \ln \frac{q^{+} - p_1^{+}}{p_2^{+}} + \frac{q^{+2}}{2p_1^{+2}} \ln \frac{q^{+}}{p_{12}^{+}} \\ + \frac{(p_{12}^{+} - q^{+})^2}{2p_2^{+2}} \left(\ln \frac{p_{12}^{+} - q^{+}}{p_2^{+}} - 1 \right) - \frac{q^{+}(p_{12}^{+} - q^{+})}{2p_1^{+}p_2^{+}} & \text{for } q^{+} > p_1^{+} \end{cases} \quad (130)$$

$$\int dx \ln x(1-x-y) = \begin{cases} \frac{q^{+}}{p_1^{+}} \left(\ln \frac{q^{+}}{p_1^{+}} - 2 \right) + \frac{p_{12}^{+} - q^{+}}{p_2^{+}} \ln \frac{p_{12}^{+} - q^{+}}{p_{12}^{+}} \\ - \frac{p_{12}^{+}(p_1^{+} - q^{+})}{p_1^{+}p_2^{+}} \ln \frac{p_1^{+} - q^{+}}{p_1^{+}} & \text{for } q^{+} < p_1^{+} \\ \frac{p_{12}^{+} - q^{+}}{p_2^{+}} \left(\ln \frac{p_{12}^{+} - q^{+}}{p_{12}^{+}} + \ln \frac{p_{12}^{+} - q^{+}}{p_2^{+}} - 2 \right) & \text{for } q^{+} > p_1^{+} \end{cases} \quad (131)$$

$$\int dx x \ln(x(1-x-y)) = \begin{cases} \frac{q^{+2}}{2p_1^{+2}} \left(\ln \frac{q^{+}}{p_1^{+}} - 1 \right) + \frac{(p_{12}^{+} - q^{+})^2}{2p_2^{+2}} \ln \frac{p_{12}^{+} - q^{+}}{p_{12}^{+}} - \frac{q^{+}(p_{12}^{+} - q^{+})}{2p_1^{+}p_2^{+}} \\ - \frac{p_{12}^{+}(p_1^{+} - q^{+})}{2p_1^{+}p_2^{+}} \left[\frac{q^{+}}{p_1^{+}} + \frac{p_{12}^{+} - q^{+}}{p_2^{+}} \right] \ln \frac{p_1^{+} - q^{+}}{p_1^{+}} & \text{for } q^{+} < p_1^{+} \\ \frac{(p_{12}^{+} - q^{+})^2}{2p_2^{+2}} \left(\ln \frac{p_{12}^{+} - q^{+}}{p_{12}^{+}} + \ln \frac{p_{12}^{+} - q^{+}}{p_2^{+}} - 2 \right) & \text{for } q^{+} > p_1^{+} \end{cases} \quad (132)$$

$$\int dx \ln y(1-x-y) = \begin{cases} \frac{q^{+}}{p_1^{+}} \left(\ln \frac{q^{+}}{p_{12}^{+}} - 2 \right) + \frac{p_{12}^{+} - q^{+}}{p_2^{+}} \ln \frac{p_{12}^{+} - q^{+}}{p_{12}^{+}} \\ - \frac{p_{12}^{+}(p_1^{+} - q^{+})}{p_1^{+}p_2^{+}} \ln \frac{p_1^{+} - q^{+}}{p_1^{+}} & \text{for } q^{+} < p_1^{+} \\ \frac{q^{+}}{p_1^{+}} \ln \frac{q^{+}}{p_{12}^{+}} + \frac{p_{12}^{+} - q^{+}}{p_2^{+}} \left(\ln \frac{p_{12}^{+} - q^{+}}{p_{12}^{+}} - 2 \right) \\ - \frac{p_{12}^{+}(q^{+} - p_1^{+})}{p_1^{+}p_2^{+}} \ln \frac{q^{+} - p_1^{+}}{p_2^{+}} & \text{for } q^{+} > p_1^{+} \end{cases} \quad (133)$$

$$\int dx x \ln(y(1-x-y)) = \begin{cases} \frac{q^{+2}}{2p_1^{+2}} \left(\ln \frac{q^{+}}{p_{12}^{+}} - 2 \right) + \frac{(p_{12}^{+} - q^{+})^2}{2p_2^{+2}} \ln \frac{p_{12}^{+} - q^{+}}{p_{12}^{+}} - \frac{q^{+}(p_{12}^{+} - q^{+})}{2p_1^{+}p_2^{+}} \\ - \frac{p_{12}^{+}(p_1^{+} - q^{+})}{2p_1^{+}p_2^{+}} \left[\frac{q^{+}}{p_1^{+}} + \frac{p_{12}^{+} - q^{+}}{p_2^{+}} \right] \ln \frac{p_1^{+} - q^{+}}{p_1^{+}} & \text{for } q^{+} < p_1^{+} \\ \frac{q^{+2}}{2p_1^{+2}} \ln \frac{q^{+}}{p_{12}^{+}} + \frac{(p_{12}^{+} - q^{+})^2}{2p_2^{+2}} \left(\ln \frac{p_{12}^{+} - q^{+}}{p_{12}^{+}} - 2 \right) - \frac{q^{+}(p_{12}^{+} - q^{+})}{2p_1^{+}p_2^{+}} \\ - \frac{p_{12}^{+}(q^{+} - p_1^{+})}{2p_1^{+}p_2^{+}} \left[\frac{q^{+}}{p_1^{+}} + \frac{p_{12}^{+} - q^{+}}{p_2^{+}} \right] \ln \frac{q^{+} - p_1^{+}}{p_2^{+}} & \text{for } q^{+} > p_1^{+} \end{cases} \quad (134)$$

References

- [1] G. 't Hooft, *Nucl. Phys.* **B72** (1974) 461.
- [2] K. Bardakci and C. B. Thorn, *Nucl. Phys.* **B626** (2002) 287, hep-th/0110301.

- [3] J. M. Maldacena, *Adv. Theor. Math. Phys.* **2** (1998) 231-252, hep-th/9711200.
- [4] C. B. Thorn, *Nucl. Phys. B* **699** (2004) 427 [arXiv:hep-th/0405018].
- [5] C. B. Thorn, *Nucl. Phys. B* **637** (2002) 272 [arXiv:hep-th/0203167].
- [6] C. B. Thorn, *Phys. Rev. D* **20** (1979) 1934.
- [7] R. J. Perry, A. Harindranath and W. M. Zhang, *Phys. Lett. B* **300** (1993) 8.
- [8] R. Giles and C. B. Thorn, *Phys. Rev. D* **16** (1977) 366.
- [9] A. Casher, *Phys. Rev. D* **14** (1976) 452.
- [10] C. B. Thorn, *Phys. Lett. B* **70** (1977) 85, *Phys. Rev. D* **17** (1978) 1073.
- [11] E. Witten, *Commun. Math. Phys.* **252** (2004) 189 [arXiv:hep-th/0312171].
- [12] F. Cachazo, P. Svrcek and E. Witten, *JHEP* **0410** (2004) 074 [arXiv:hep-th/0406177].
- [13] S. J. Parke and T. R. Taylor, *Phys. Rev. Lett.* **56** (1986) 2459.
- [14] C. B. Thorn, “Notes on One-loop Calculations in Light-cone Gauge,” arXiv:hep-th/0507213.
- [15] Zvi Bern, private communication.
- [16] Z. Bern and D. A. Kosower, *Nucl. Phys. B* **379** (1992) 451.
- [17] Z. Kunszt, A. Signer and Z. Trocsanyi, *Nucl. Phys. B* **411** (1994) 397 [arXiv:hep-ph/9305239].
- [18] Z. Bern, L. J. Dixon and D. A. Kosower, arXiv:hep-ph/0507005.
- [19] K. Bering, J. S. Rozowsky and C. B. Thorn, *Phys. Rev. D* **61** (2000) 045007 [arXiv:hep-th/9909141].